Eindhoven University of Technology

BACHELOR

Solution deposition of matter on a hydrophobic substrate by infrared irradiation

Scheerder, R.W.H.S.

Award date:
2014

Link to publication

Disclaimer
This document contains a student thesis (bachelor's or master's), as authored by a student at Eindhoven University of Technology. Student theses are made available in the TU/e repository upon obtaining the required degree. The grade received is not published on the document as presented in the repository. The required complexity or quality of research of student theses may vary by program, and the required minimum study period may vary in duration.

General rights
Copyright and moral rights for the publications made accessible in the public portal are retained by the authors and/or other copyright owners and it is a condition of accessing publications that users recognise and abide by the legal requirements associated with these rights.

- Users may download and print one copy of any publication from the public portal for the purpose of private study or research.
- You may not further distribute the material or use it for any profit-making activity or commercial gain

Technische Universiteit
Eindhoven
University of Technology

Report of the BSc-final project

Solution deposition of matter on a hydrophobic substrate by infrared irradiation

by

R.W.H.S. Scheerder

Student number: 0776513

Date: 06-07-2014

Supervisor: MSc H.M.J.M Wedershoven

Mesoscopic Transport Phenomena Group

Abstract

The goal of the project is to study solution deposition of materials on a substrate with the help of an infrared laser. We want to deposit matter on a substrate by mixing it in an volatile fluid and inducing heat into the mixture and substrate with an infrared laser. This way we would like to precisely deposit the matter on a substrate by deforming and evaporating the solvents. If we move the substrate we could "write" patterns with the dissolved materials. This technique is a sort of lithographic process and can be used in this field of work, thinking about creating semiconductor devices ('chips') or OLED screens[1].

The absorption of the laser power results in a non-uniform temperature distribution, this causes deformation of the thin liquid film. The effects of different parameters such as laser power, initial film thickness and concentration of dissolved matter are studied as well as the effect of the speed of motion of the substrate.

We use an initial layer of the mixture that is typically a couple of microns thick. If we're going to look at the deposition of matter (we use PVPS (Poly(1-vinylpyrrolidone-co-styrene)) as a model in the solution) on a stationary substrate we can see that increasing laser power causes an increase in size of the deposition. Increasing initial film thickness seems to cause decreasing size of deposition. But relative to the increase effect of the laser power this seems negligible. The tested concentration of matter (10% and 15%) also don't seem to make a difference in the size of deposition.

With a stationary substrate we also mapped the time dependence of the process, the size of the deposition is laid out against the time. Here the results show that with higher laser power the actual deposition starts earlier but the increase in size over time doesn't depend on any of the studied parameters.

Next is the 'lithographic process' where we use a moving substrate. Here we see the same relation between the laser power and the track width of the deposition; increasing power causes increasing width. The initial film thickness causes no significant differences in track width, just so as a different concentration of matter. Now if the speed of motion is altered we measure that with an increasing speed the track width will decrease. Before a measurement was labeled as 'successful' the criterion, that a steady state was reached during the measurement, needed to be fulfilled. This was not the case at certain settings where movement speed was too slow or the laser power too high.

Table of contents

1 Introduction

1.1 Literature review on deposition of matter by laser irradiation

The call for these techniques, so called 'direct-writing technologies', have been recently emerging in response to the need of continuous micro-patterns of particles. Thinking of industrial applications like inkjet printing, micropen writing or laser particle guidance. These are all relatively new techniques so the research into laser-based deposition is also relatively new, say the start of the 21st century.

By Bieri *et al.*[2] the process of printing and laser curing of nanoparticle solutions is studied. A liquid solvent is employed as the carrier of gold nanoparticles possessing a low melting temperature compared to that of bulk gold. Using a specifically designed printing system, the gold nanoparticle solution is deposited on a substrate and cured with laser radiation. In this manner, the potential of writing gold structures on temperature sensitive substrates is demonstrated. The interaction between the laser radiation and nanoparticles drives the solvent evaporation and controls the quality of the microstructures printing process. The latter is also affected by thermocapillary flow at the free surface, developing during the curing process. This leads to layers of a couple of hundred nanometers of gold particles. Later on Bieri[3] also studied a moving process where the laser is moved relatively to the substrate.

Kochemirovsky *et al.*[4] showed that alcohols with 1,2,3,5,6 hydroxyl groups can be used as reducing agents for laser-induced copper deposition from solutions (LCLD). Multiatomic alcohols, sorbitol, xylitol, and glycerol, are shown to be effective reducing agents for performing LCLD at glass-ceramic surfaces. High-conductivity copper tracks with good topology were synthesized. The work determines the regularity of changes in properties of metallic deposits depending on the reducing potential of the polyol.

Nadgorny *et al.*[5] demonstrated that the laser-based particle deposition (LBPD) technique makes it possible to deposit a variety of materials at the micron scale in the form of individual particles or clusters, with the particle size ranging from tens of nanometers to less than a micron. A weakly focused, relatively low-power laser beam guides micron-sized droplets through a micron-sized aperture toward a substrate after the droplets are generated by an atomizer from a liquid precursor or a suspension of particles. The technique allows depositing, codepositing, and patterning materials of different classes making use of the same basic fabrication technology. Another essential asset of the technique is that the light– matter interaction inside the LBPD apparatus allows controllable activation of the chemical reactions and/or phase transformations inside the droplets making the technique even more flexible.

In this project, the goal is to use a technique on a thin film of a certain solution spread out on a hydrophobic substrate a couple of centimeters wide and long. The deposition is on the micron scale and the influences of the process parameters itself are more the focus of the study than the material parameters.

1.2 Thermocapillary flow

The principle of the experiments is based on is thermocapillary deformation. If the thin film is treated with the laser there will be absorption of the laser power, which produces heat.

First an approximation is made that describes how a thin liquid film deforms under the action of a temperature gradient. After that the temperature profile of a thin liquid film is coupled to that of a laser-heated substrate onto which it is applied. This results in a numerical model for a stationary and moving substrate. The derivation is done in [6]. Although we are not interested in the deformation of the film itself, we can still use some relations between parameters to predict or explain some behaviors.

Figure (1) shows a schematic image of a thin liquid film on a laser heated substrate. The system is axisymmetric and the axis is shown in the figure. The thickness of the film is not to scale compared to the thickness of substrate.

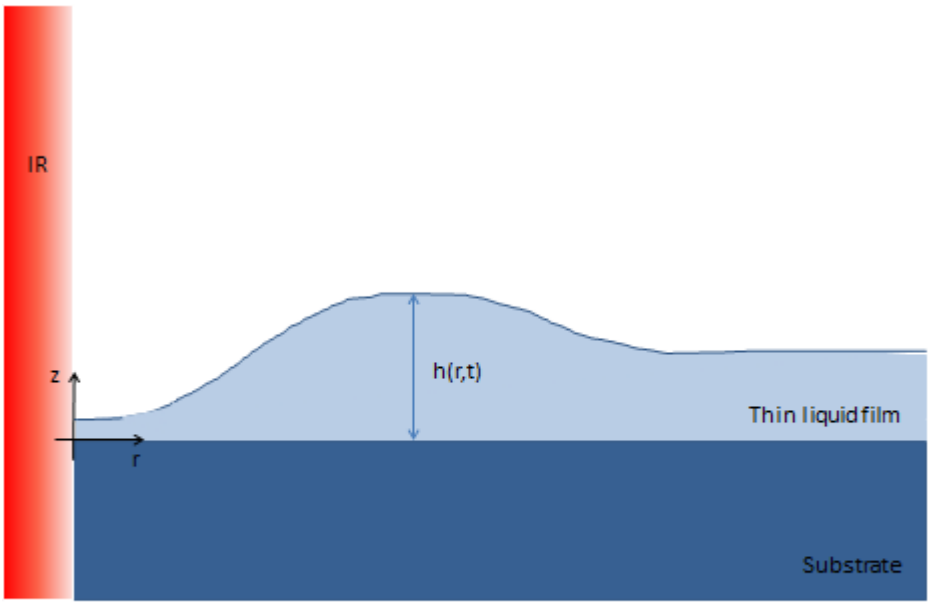

Figure 1: Schematic image of a thin liquid film on a substrate heated by a laser beam.

The starting point is the Navier-Stokes equation and the continuity equation for an axisymmetric flow without swirl in a cylindrical system.

$$\rho\left(\frac{\partial u_r}{\partial t}+u_r\frac{\partial u_r}{\partial r}+u_z\frac{\partial u_r}{\partial z}\right)=-\frac{\partial P}{\partial r}+\mu\left(\frac{1}{r}\frac{\partial}{\partial r}\left(r\frac{\partial u_r}{\partial r}\right)+\frac{\partial^2 u_r}{\partial z^2}-\frac{u_r}{r^2}\right) \quad (1)$$

$$\rho\left(\frac{\partial u_z}{\partial t}+u_r\frac{\partial u_z}{\partial r}+u_z\frac{\partial u_z}{\partial z}\right)=-\frac{\partial P}{\partial z}+\mu\left(\frac{1}{r}\frac{\partial}{\partial r}\left(r\frac{\partial u_z}{\partial r}\right)+\frac{\partial^2 u_z}{\partial z^2}\right) \quad (2)$$

$$\frac{1}{r}\frac{\partial}{\partial r}(ru_r)+\frac{\partial u_z}{\partial z}=0. \quad (3)$$

Here equations (1) and (2) describe the conservation of momentum in the *r*- and *z*-direction. u_r is the velocity of the liquid in the *r*-direction, u_z is the velocity in the

z-direction. P is the dynamic pressure defined as $P = p + \rho g z$, where p is the pressure in the liquid. Equation (3) describes the conservation of mass. ρ and μ are respectively the density and viscosity of the liquid.

After the derivation made in [6] a relation has been found that describes the evolution of the thin liquid film profile $h(r,t)$. Some assumptions have been made to simplify with regard to relative magnitude. In the thin film equation the characteristic magnitude of the length is much bigger than that of the height. Here the initial film thickness $h_0 \approx 5\mu m$ is much smaller than the diameter of the laser spot $w = 120\mu m$. Now the relation is given by:

$$\frac{\partial h}{\partial t} + \frac{1}{r}\frac{\partial}{\partial r}\left(r\left(\frac{h^2}{2\mu}\frac{\partial \sigma}{\partial r} - \frac{h^3}{3\mu}\frac{\partial P}{\partial r}\right)\right) = 0 \tag{4}$$

$$P = -\frac{\sigma}{r}\frac{\partial}{\partial r}\left(r\frac{\partial h}{\partial r}\right) + \rho g z$$

where the temperature profile at the liquid-air interface enters equation (4) through the shear stress term $\frac{\partial \sigma}{\partial r}$, since the surface tension depends on the temperature. This term can therefore be written as $\frac{\partial \sigma}{\partial r} = \frac{\partial \sigma}{\partial T}\frac{\partial T}{\partial r}$. The term $\frac{\partial \sigma}{\partial T}$ is assumed a constant.

For a moving substrate some alterations have been made. The substrate now moves in the positive y-direction with a velocity U. This results in the following expression:

$$\frac{\partial h}{\partial t} + \frac{\partial}{\partial x}\left(\frac{h^2}{2\mu}\frac{\partial \sigma}{\partial x} - \frac{h^3}{3\mu}\frac{\partial P}{\partial x}\right) + \frac{\partial}{\partial y}\left(\frac{h^2}{2\mu}\frac{\partial \sigma}{\partial y} - \frac{h^3}{3\mu}\frac{\partial P}{\partial y} + Uh\right) = 0 \tag{5}$$

$$P = -\sigma\left(\frac{\partial^2 h}{\partial x^2} + \frac{\partial^2 h}{\partial y^2}\right) + \rho g h.$$

Now the next process included in the model is the heating of the substrate by the laser. Here the effect of a heated substrate is applied on the thin film. We will study how the temperature profile at the liquid-air interface is related to the temperature profile at the top surface of a laser-heated substrate.
Only the heating of the substrate has been included in this model because the heat source in the liquid is assumed negligible. The axisymmetric heat transfer equation in cylindrical coordinates is

$$\frac{1}{r}\frac{\partial}{\partial r}\left(r\frac{\partial T}{\partial r}\right) + \frac{\partial^2 T}{\partial z^2} + \frac{1}{k}g(r,z) = \frac{1}{\alpha}\frac{\partial T}{\partial t}. \tag{6}$$

T represents the temperature, k the thermal conductivity of the substrate and α its thermal diffusivity. Now g is the represents a source of heat due to absorption of the laser intensity by the substrate. It can be calculated by multiplying the local intensity $I(r,z)$ with the absorption coefficient γ of the substrate.

Now we have got the relation between the laser intensity and the temperature profile of the substrate (linear). And [6] shows that, under the assumption that the film thickness is much smaller than the substrate thickness, the heat flux at the liquid-air interface is continuous and given by

$$T_2 - T_1 = \frac{h_{N,liq} d_{liq}}{k_{liq}}(T_1 - T_0)\ . \tag{7}$$

Here T_0 is the temperature of the surrounding air, T_1 the temperature at the liquid-air interface, T_2 the temperature at the substrate top and liquid interface and $h_{N,liq}$, d_{liq},

k_{liq} respectively the convective heat transfer coefficient, the liquid film thickness and the heat conduction coefficient. The last three are material constants. So the relation between the laser intensity and the thickness is assumed linear.

A process that also plays a part in practice is evaporation. The effects of this process are not included in the numerical model described above.

2 Experimental set-up

2.1 Set-up

To accomplish the experiment we used the setup shown in figure (2). The crucial components are a spin coater, an infrared laser and a camera.

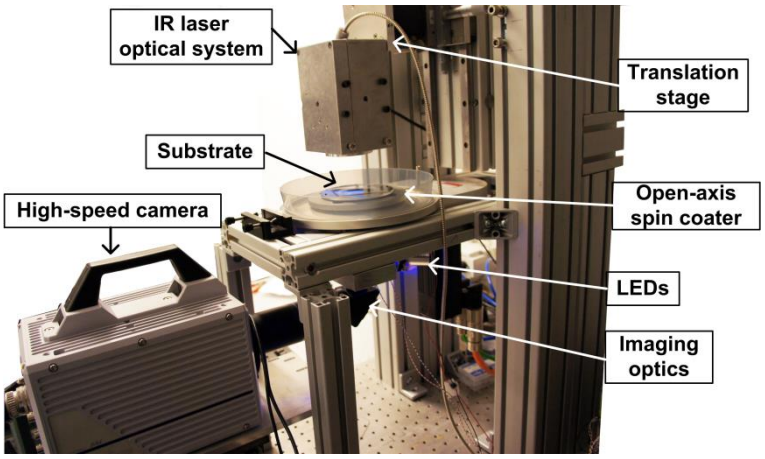

Figure 2: A picture of the real set-up used to do the experiments. The components are named in the picture.

The substrates that are used are polycarbonate substrates that are $750\ \mu m$ thick. These are hydrophobic for water and ethylene glycol, the solvents used in the experiments. We can make these substrates hydrophilic so that the liquids are wetting on the surface, this can be done by cleaning them by means of a UV-ozone treatment.

First let's clarify the difference between hydrophobic and hydrophilic. A liquid on a solid surface can be hydrophilic or hydrophobic depending on the intermolecular interactions of these two materials. The relative magnitude of the adhesive and cohesive forces determine the angle at which the liquid will border on the solid; the contact angle. If this contact angle is very low, going to zero, the liquid is wetting on the surface which is called hydrophilic. At larger contact angles the surface is called partially-wetting and hydrophobic.

The cleaning of the substrates is done by first placing the polycarbonate in a UV-cleaner and then washing them off with distillated water which renders them completely wetting. (The UV-ozone treatment oxidizes, i.e. chemically modifies the chemical composition of the surface).

There is also need of hydrophobic substrates where the dewetting process of the liquid on the substrate is delayed so that the laser has longer time to work. This can be accomplished by placing a mask on the polycarbonate plate when placed in a UV-cleaner, as shown in figure (3). The cleaning process from the UV-cleaner doesn't affect the surface covered by this mask. Now there is a hydrophilic circle surrounding the hydrophobic center that delays the dewetting process by keeping de film in place around the circle contour for a while.

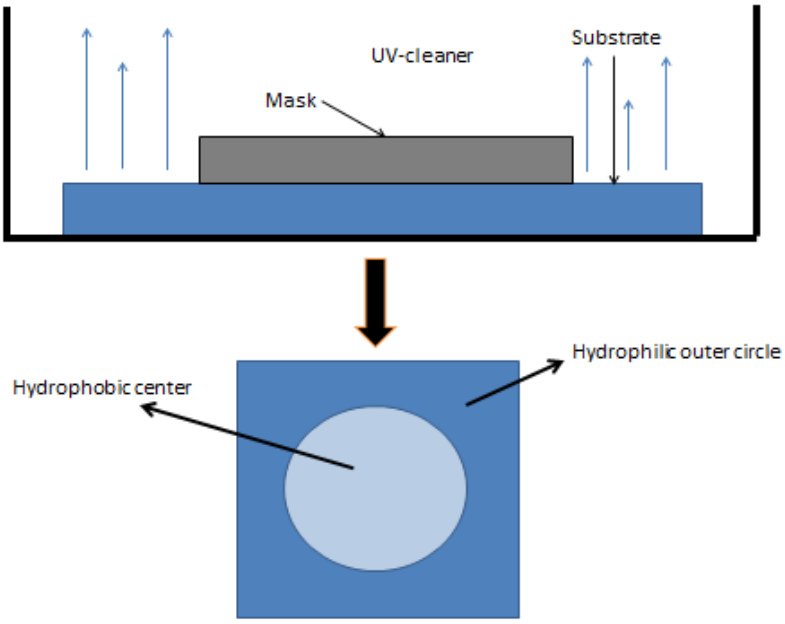

Figure 3: A schematic image of the UV-cleaning process. A mask is placed on the substrate to leave the center hydrophobic.

A couple of milliliters of liquid are deposited on the substrate and the spin-coater spins the substrate with the liquid at a very high rotation speed. Thus spreading out the liquid over the substrate with a uniform thickness. The spin-coater is integrated in the system and is adjustable in *rpm* (rounds per minute) and spin-coating time *t*. Hereby we can create different thicknesses of films on the substrate. Figure (4a) illustrates the spin-coating process.

2.2 Laser treatment

After the thin film is created the laser induction begins, meaning the laser is switched on. The laser source is a fiber-coupled laser diode from Lumics (model number LU1470C020-C) and has a maximum output power of *20W*. The wavelength of this infrared laser is *1470 nm*. The laser light is coupled into an optical fiber, the output side/end which is placed a couple of centimeters above the substrate. The light is focused into a spot diameter of $120\mu m$ on the substrate surface by means of an optical lens system. The power of the laser beam can be increased by increasing the operating current of the laser. However, this does not increase linear and therefor a duty cycle signal with a high frequency modulates the power at a fixed operating current.

When the substrate and liquid film are heated, the gradient in temperature causes a gradient in surface tension along the liquid-air interface. Thus, the liquid will move away from the laser spot. It could be heated as much that the liquid or solvent even starts the evaporate. When a mixture is used the dissolved particles will precipitate on the substrate, where the solvent evaporates, and leave a layer behind. Thus we have three processes. The total process is depicted in figure (4b).

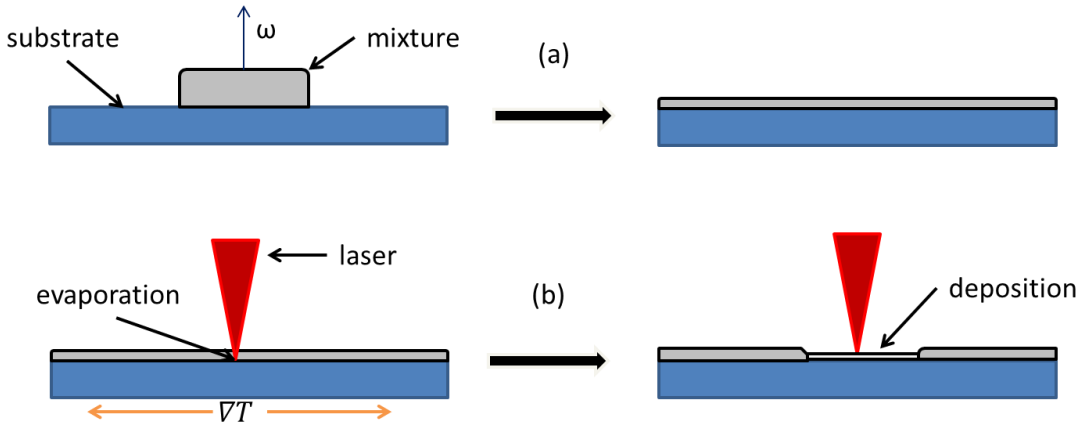

Figure 4: A schematic image of (a) the spin-coating, (b) laser heating and deposition process on a stationary substrate.

When we want to study the behavior of the effects on a moving substrate the laser spot is moved out of the center of the substrate, which is the axis of rotation in the spin-coating process. After the spin-coating process the polycarbonate plate rotates with a constant angular velocity, much slower than the spin-coating speed. The laser is switched on and deposits a track of matter along a circular line. The track can be seen as a straight track if the radius of the circle from the center of the substrate to the deposited track is much bigger than the diameter of the laser spot, which is the case. After the track reaches a length a couple times bigger than the diameter of the laser spot a steady state has been reached, which is when the track stays of a uniform width. From here we can study the track after the dewetting phase. This process is shown in figure (5).

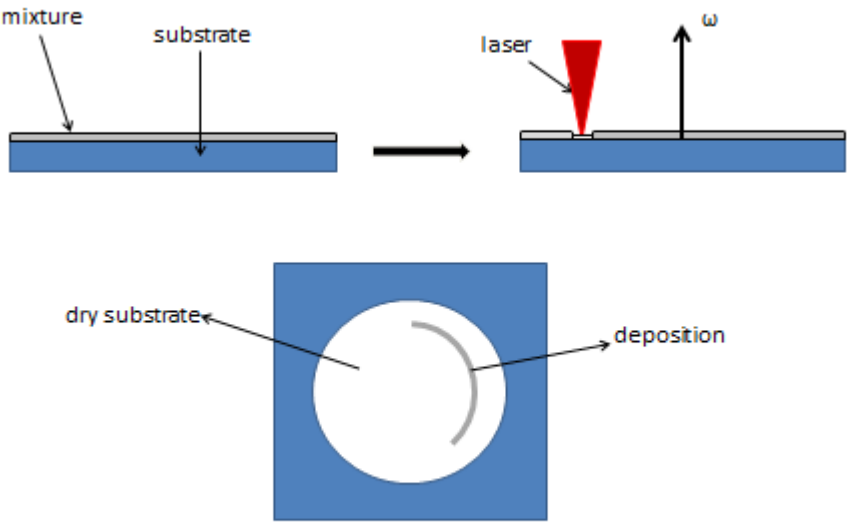

Figure 5: A schematic image of the laser heating and deposition process on a moving substrate.

2.3 Observing with dual-wavelength interferometry

The deformation of the thin film is visualized using dual-wavelength interferometry. This principle rests on constructive and destructive interference of the light emitted by a LED. Two different LEDs with different wavelengths, one with a wavelength of $\lambda_R = 625\,nm$, the other with $\lambda_B = 466\,nm$, are used. The images are recorded on a CCD camera (Photron fastcam SA4, model: 500K-M1).

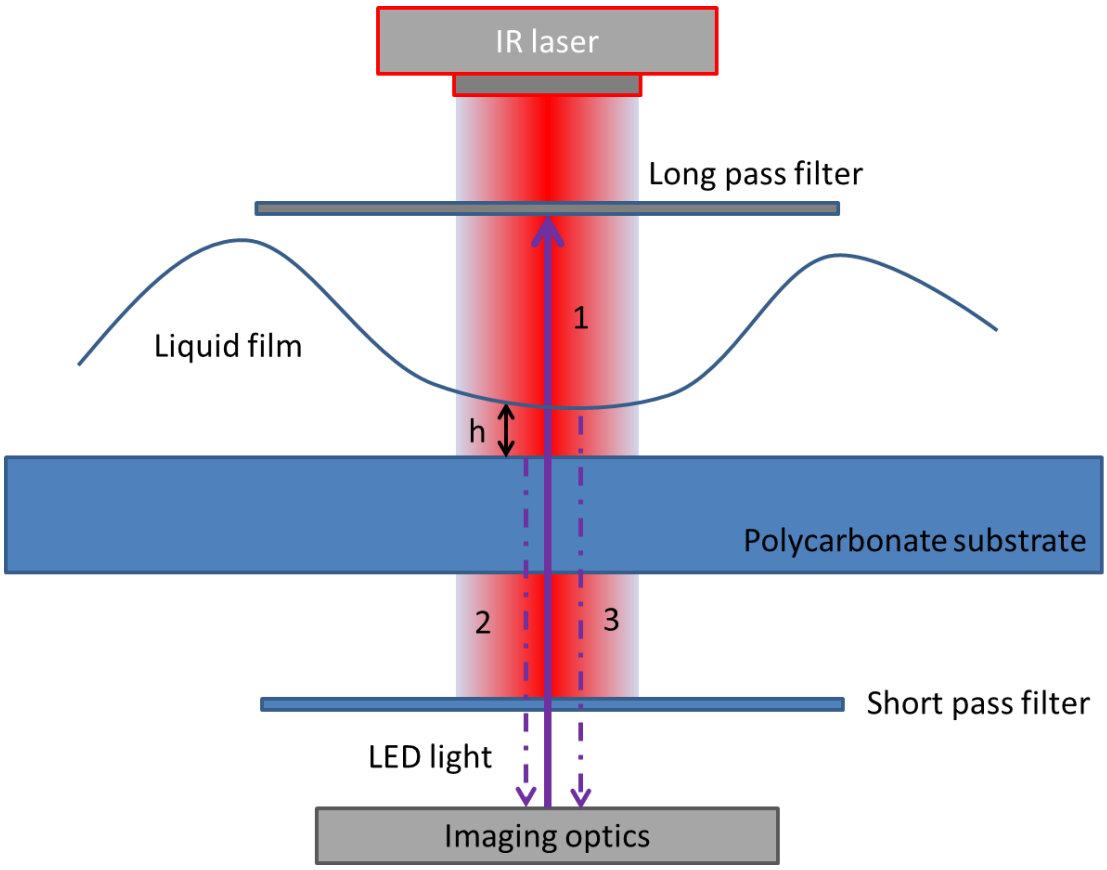

Figure 6: A schematic image of the used imaging technique. The components are named and numbered.

The light from the LEDs is emitted upwards from underneath the substrate through a short pass filter. It is then transmitted through and reflected by the substrate and liquid film. Now the light from the LEDs is blocked by a long pass filter (Optical cast plastic infrared long pass filter, Edmund Optics 43-949). Is this filter isn't placed, the light from the LEDs would enter the optical system for the focusing of the infrared laser beam. This system would then partially reflect and focus these light rays. This would disturb the image of the interference between the reflection from the liquid film and the substrate.

Rays '2' and '3' will now interfere. Since they travelled a different optical path their phase will be different. This optical path length difference is given by $2nh$, where n is the refractive index of the liquid and h is the local film thickness. Where $2nh = m\lambda$ (where m is an integer and λ the used wavelength) there will be constructive interference and when $2nh = (m + \frac{1}{2})\lambda$ there will be destructive interference. In figure (7) we can see the different interference patterns of the two used LEDs.

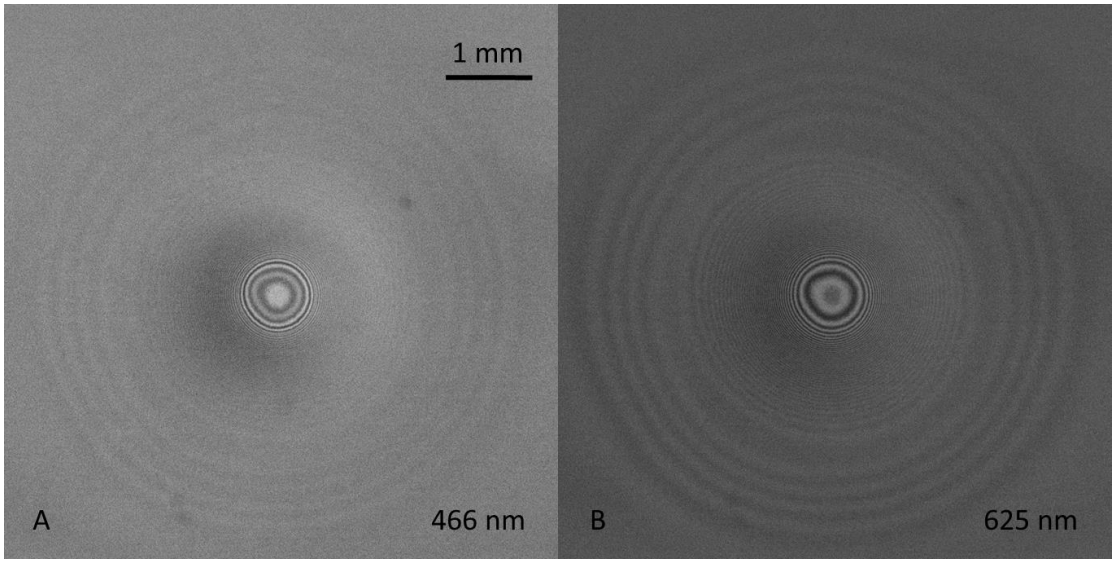

Figure 7: Interferometry images of the thin film deformation (A: $\lambda = 466\ nm$, B: $\lambda = 625\ nm$).

By noting the positions of all light and dark fringes and by using the fact that the difference in film thickness between a light and dark fringe is constant, namely $\lambda \backslash 4n$, it is possible to construct a profile of the relative film thickness. However, when this is measured for two different wavelengths, an absolute thickness h could be determined.

Because the refractive index of volatile solutions changes with composition, we did not attempt to extract film thickness distributions, but just used the imaging setup for visualization.

With a similar method the thickness of a liquid film can be determined. It has been done, as we will see later in this report, but with a different set-up based on the same principle. Here a whole spectrum is used instead of two wavelengths.

3 Break-up of a thin liquid film

Before we are going to look at depositing matter on a substrate, we are going to look at the behavior of just the pure solvent. When the thin film of liquid is exposed to the laser the film is being deformed. A flow will be induced under the action of an applied temperature gradient. This is called the thermocapillary deformation as described in paragraph 1.2.

Due to this thermocapillary flow the film will draw away from the laser spot and due to the heating the liquid will evaporate. On a hydrophilic substrate this will result in a dry spot. On a hydrophobic substrate the film will reach a minimum thickness and will break-up. The two different cases are depicted in figures 8 and 9 for an ethylene glycol film.

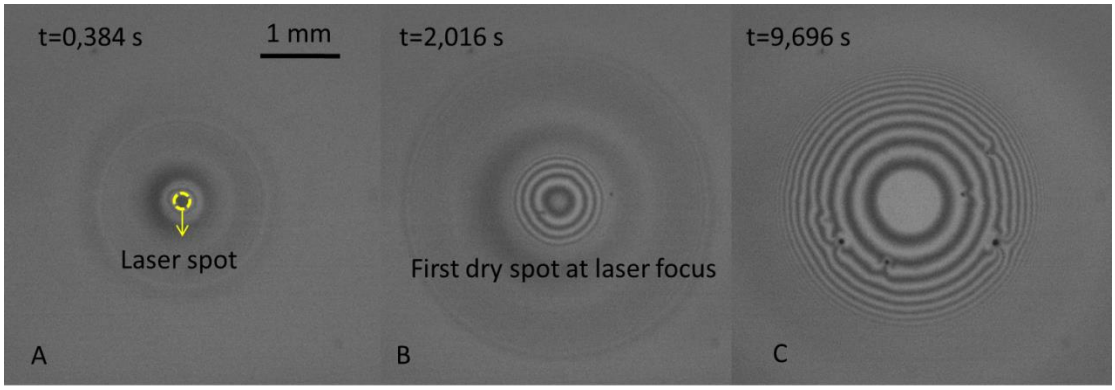

Figure 8: Deformation of a thin ethylene glycol film on a hydrophilic substrate. At panel B a first dry spot at the center of the focus can be observed, this will grow over time (see panel C).

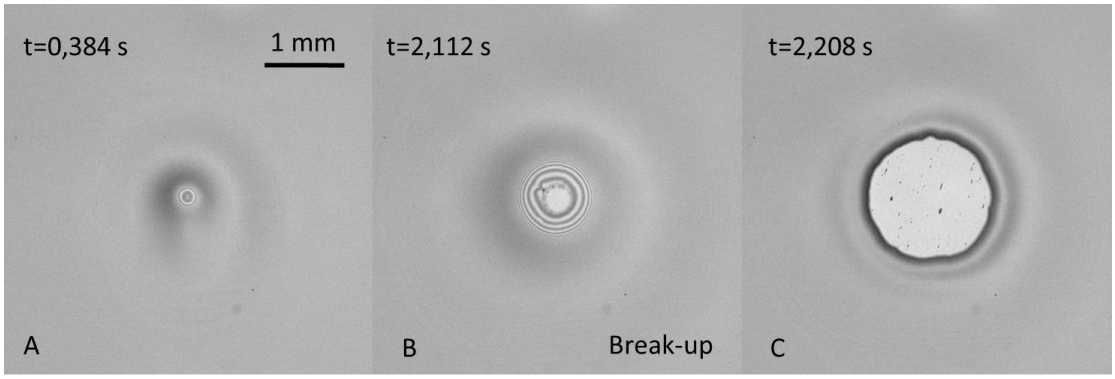

Figure 9: Deformation of a thin ethylene glycol film on a hydrophobic substrate. At panel B break-up and dewetting occurs.

The time at which this occurs is called the rupture time. From the measurements, this time is calculated by determining the time when the greyscale of the center of deformation doesn't change anymore. After the break-up we can see that the hydrophobic substrate dewets completely in contrast to the hydrophilic. Here the dry spot in the center doesn't grow after the 10 seconds of laser induction and stays for minutes after.

The rupture time is studied at different laser powers on hydrophilic and hydrophobic substrates and with different liquids. The liquids used are water and ethylene glycol.

3.1 Rupture time as a function of laser power: hydrophobic and hydrophilic substrates

First we look at the behavior of the deformation and, more precise, the rupture time of ethylene glycol on a hydrophobic and a hydrophilic substrate. This to see what differences it brings to the experiments on a hydrophobic substrate.

In figure (10) below the rupture times of the hydrophilic substrates are plotted against the laser power on a logarithmic scale, in figure (11) the same is done for a hydrophobic substrate.

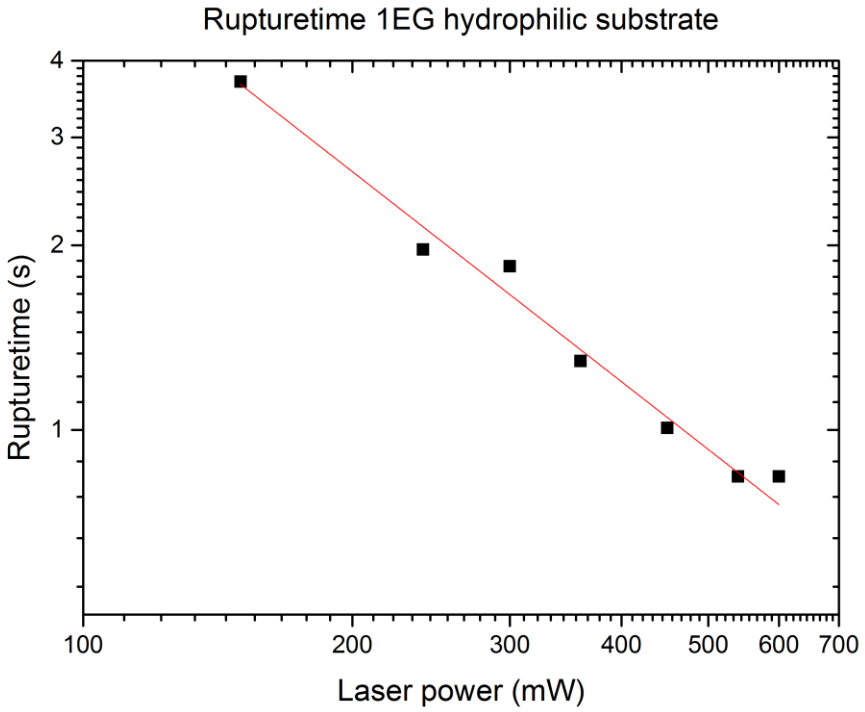

Figure 10: Plot of the rupture time against the laser power of 1EG on a hydrophilic substrate. Spin-coating happened for 5 seconds on 2000 rpm. The fit through the results is $t_r=1096{,}54P^{-1{,}138}$.

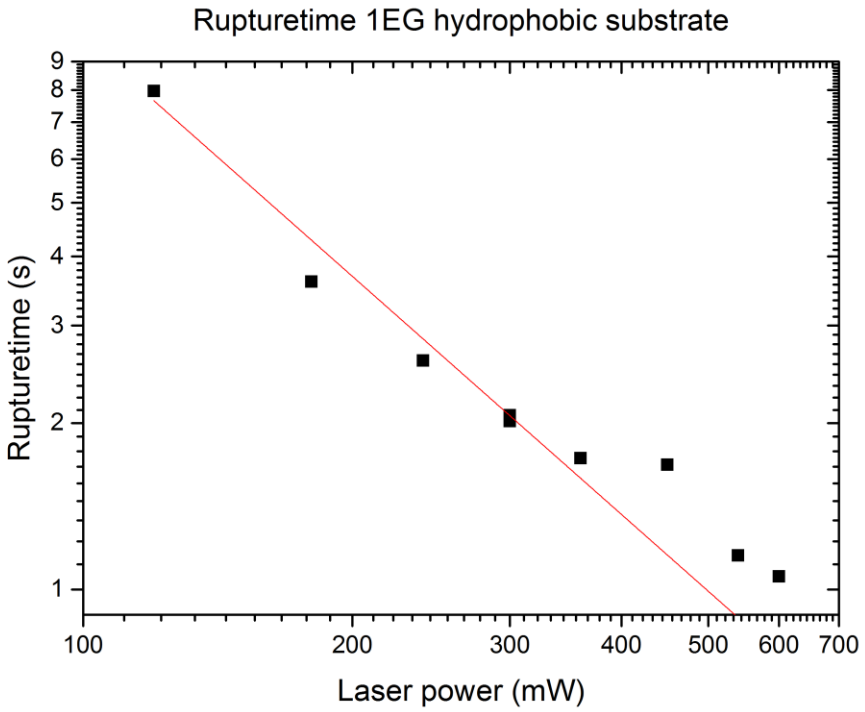

Figure 11: Plot of the rupture time against laser power of 1EG on a hydrophobic substrate. Spin-coating happened for 5 seconds on 2000 rpm. The fit through the results is $t_r=7210{,}61P^{-1{,}430}$.

For comparison, these plots are now put together in figure (12).

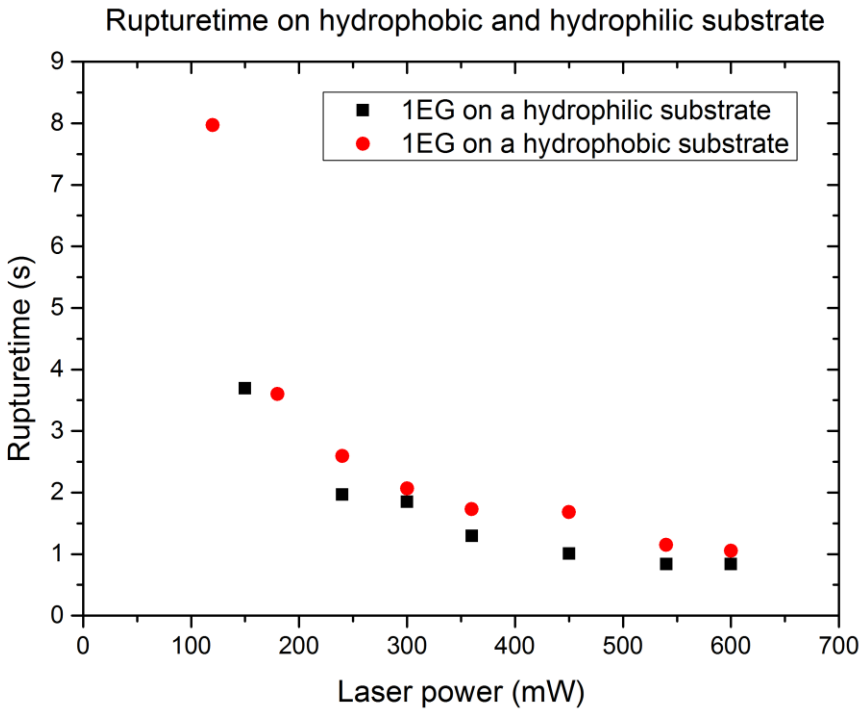

Figure 12: Compared results of the rupture time against the laser power for 1EG on hydrophilic and hydrophobic substrates.

The experiments show that it doesn't seem to matter if the substrate is hydrophobic or hydrophilic if we look at the rupture time. So it's a point that doesn't need to be taken into account. We can also see that with increasing laser power the rupturetime decreases.

3.2 Rupture time as a function of laser power: different liquids

The next parameter that is studied is the used liquid. At the previous experiments ethylene glycol is used for the film. Although the solvents used in further experiments is water. Ethylene glycol is similarly polar liquid as water, but a major difference is that water has a lower viscosity. The rupture time of water films is plotted against the laser power and is shown in figure (13).

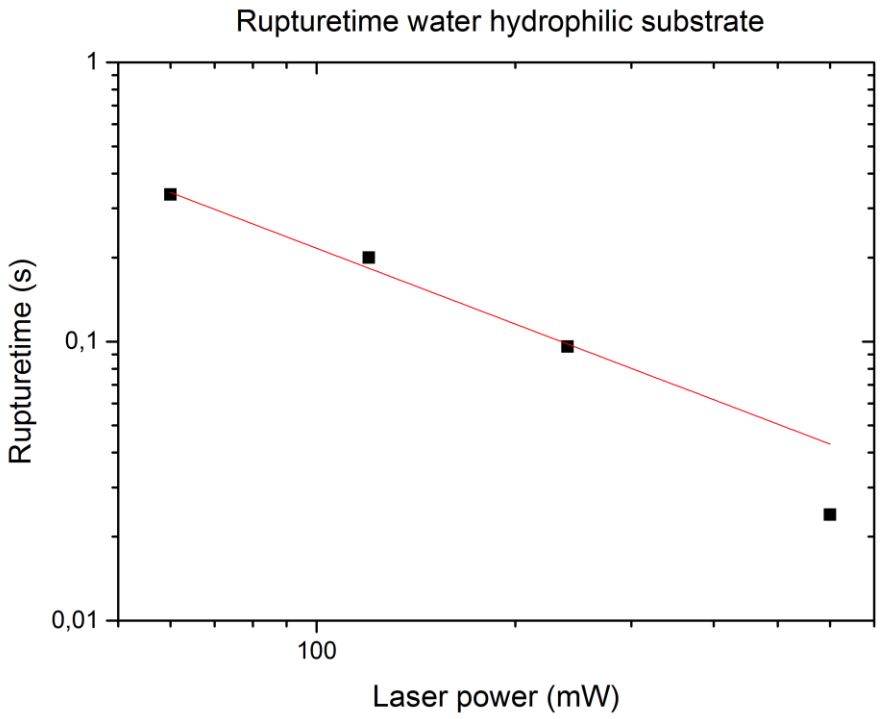

Figure 13: Plot of the rupture time against the laser power for water on a hydrophilic substrate. The fit through the results is $t_r=13{,}72P^{-0{,}902}$.

For comparison, the plot where water is used is put together with the results of ethylene glycol in figure (14).

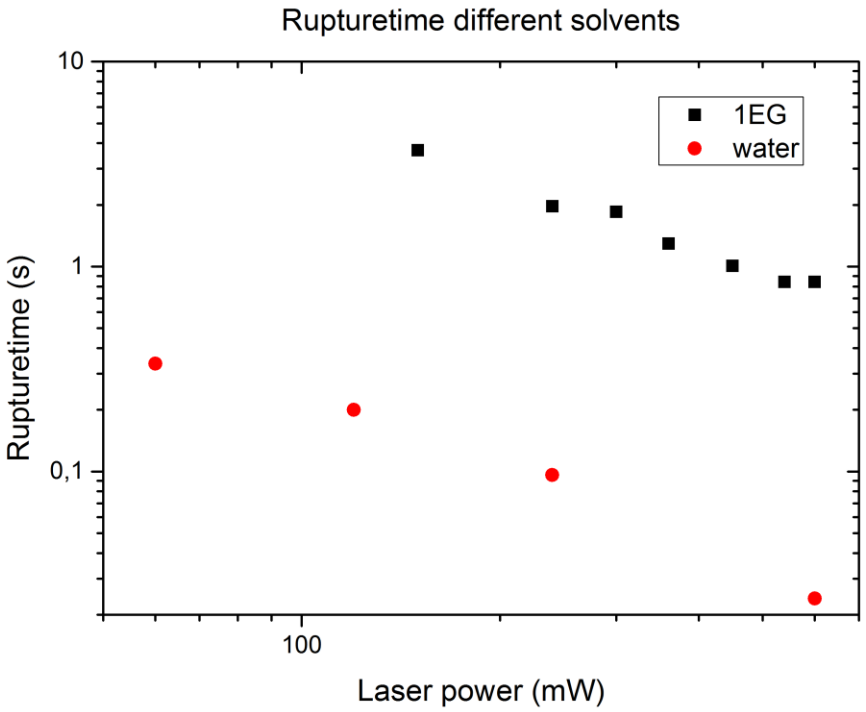

Figure 14: Compared results of the rupture time plotted against the laser power of 1EG and water on a hydrophilic substrate.

From the result we can derive that a liquid with a lower viscosity has a faster rupture time. This is consistent with the expected outcome when we look at the thin film equation (5) in paragraph 1.2. The viscosity term μ is inversely proportional to the film thickness. Water has an unpractical low viscosity, because the film will break-up too fast, but with the dissolved matter the viscosity will increase.

4 Deposition of matter on a stationary substrate

Now we come to the part of the experiment where matter is deposited on the polycarbonate plate. The mixture used is PVPS or Poly(1-vinylpyrrolidone-co-styrene) in water with a particle size of less than $0{,}5\ \mu m$. The solution used in all experiments is $10\ wt\%$ PVPS and $90\ wt\%$ water on mass base, except where noted otherwise.

A thin film of this mixture is placed on the substrate after which the laser is switched on. This will conclude in the process that is described in figure (4). Through the high speed camera this process looks like the image sequence in figure (15).

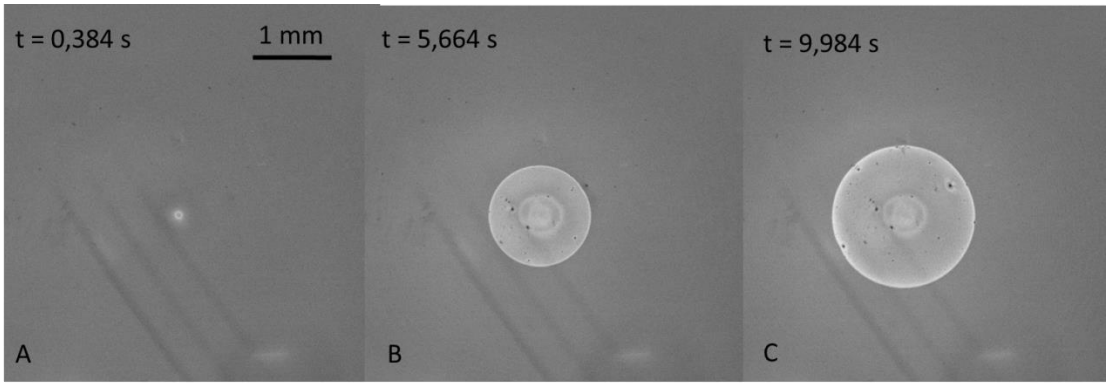

Figure 15: Image sequence of the deposition process at a laser power of 450mW. The time t=0 corresponds with the switching on of the laser.

The size of depositions are measured via the images from the high speed camera ($1\ pixel = 4{,}11 \mu m$) and, after the laser is switched off and the dewetting of the substrate has occurred, the results are looked at with a microscope. The condition before a deposition is calculated is based on the greyscale of an image. When a circle is formed, with its center at the laser spot, with a grayscale between *0,5* and *0,7* this is interpreted as a deposition of matter. This grayscale is chosen separately for every measurement depending on the contrast in the images. Every pixel is given a grayscale between *0* (white) and *1* (black). A parameter study is performed and the results are listed in the following paragraphs. For all following experiments on a stationary substrate the laser has been on for 10 seconds.

This time wasn't chosen completely at random, it has been based on the time it takes for the (hydrophobic) substrate to dewet by itself. Also, it could occur that with a high enough laser power the solution dewets at the border of the deposition before the total laser time has finished. An example is shown in figure (16).

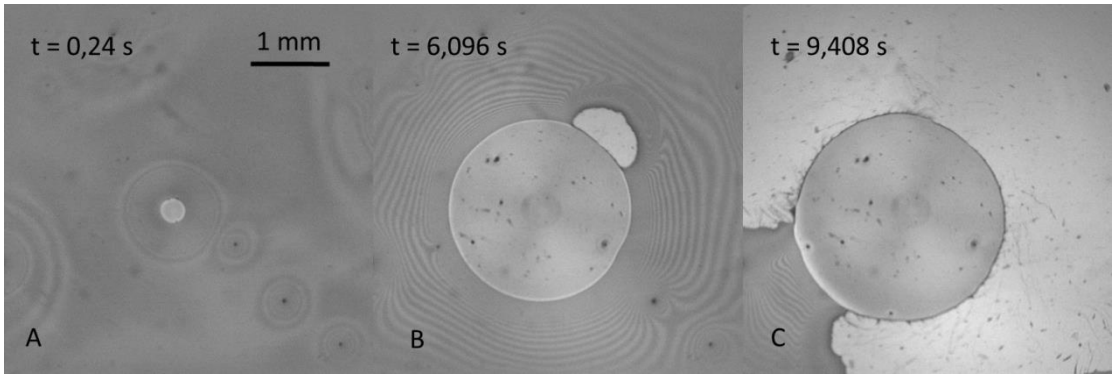

Figure 16: Image sequence of a premature break-up at the border of the deposition spot. The laser power is 1200 mW.

4.1 Deposition size as function of laser power

After the treatment with the laser heat the radius of the layer of matter is measured. The laser power varies between $60\,mW$ and $600\,mW$. After, the radius is plotted against the laser power. This is shown in figure (17).

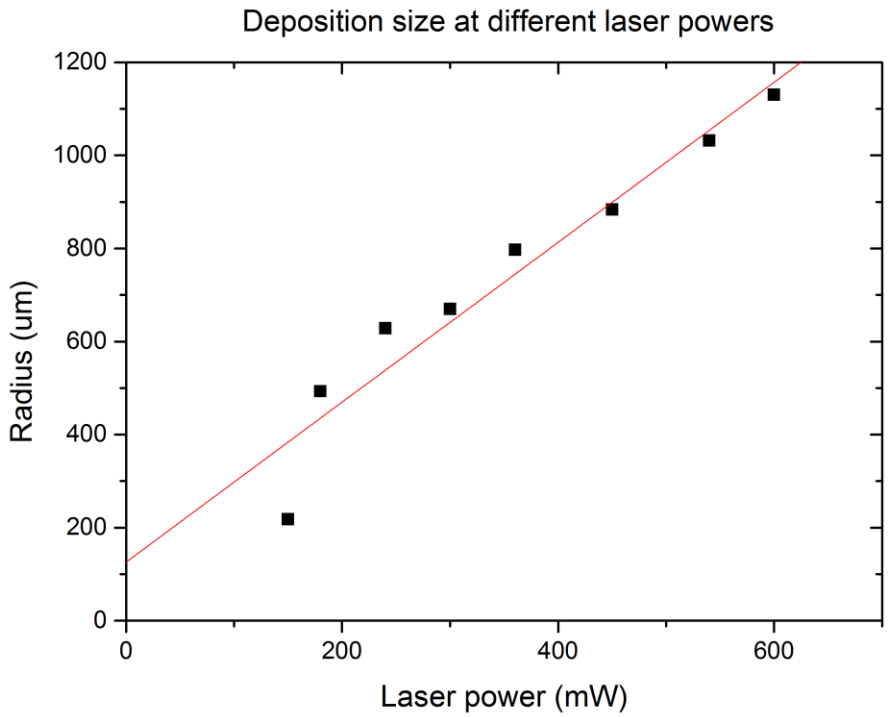

Figure 17: Plot of the radius of the deposition against the laser power, done with a 10% PVPS solution. Spin-coating is done for 2 seconds on 1500 rpm and the laser lasted for 10 seconds. The fit through the result is a linear fit with parameters R=125,83+1,718P.

From the results we can clearly see that the size of the deposition grows with increasing laser power which looks fairly linear. But at a very low laser power there has to be concluded that the size is much smaller than expected with this linear relation. Also a sort of threshold has to be crossed before actual deposition is formed.

This is the laser power for which, with a 10 second treatment, the thin film is diminished enough to a thin layer where deposition occurs.

4.2 Deposition size as function of initial film thickness

Also here the radius of the deposition is measured but now as function of the initial film thickness i.e. as function of the angular velocity during spin-coating. For the measurement of the film thickness we use. The reflection of upper and lower boundary of the film interfere with each other to get destructive and constructive interference. This is possible for pure liquids like water or ethylene glycol but not for colloidal dispersions like the PVPS in water. Here the particles interfere with the measurement due to scattering of light on these particles. This is why no absolute film thickness could be measured.

We know that for a Newtonian liquid of constant and shear-independent viscosity the thickness h decreases with $t^{-\frac{1}{2}}$ with t the spin-coating time and ω^{-1} with ω the spin-coating rpm[7]. The film thickness is inversely proportional to the angular velocity during spin-coating. But we can say that the film thickness is in the magnitude of a couple of microns, between $5\,\mu m$ and $14\,\mu m$. This information comes from the thickness measurement done on water and ethylene glycol as pure liquids.

In figure (18) we can see a plot of the radius of the deposition as function of ω. This measurement is done at two fixed laser powers, namely $180\,mW$ and $450\,mW$.

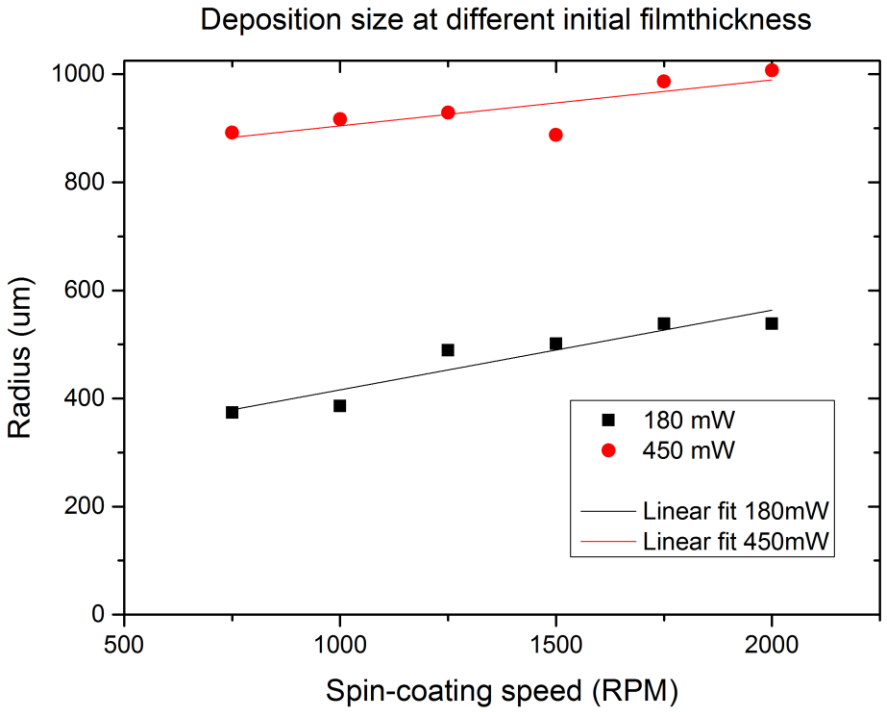

Figure 18: Plot of the radius of the deposition against the spin-coating rpm, done with a 10% PVPS solution. Compared results for a laser power of 180 mW and 450 mW, the laser was on for 10 seconds. The linear fits for 180 mW and 450 mW give respectively R=268,48+0,147P and R=819,49+0,085P.

It can be seen that the deposition size increases with a thinner film. But the difference in radius is pretty small in relation to that of the influence of the laser power.

Now we only look at the radius of the deposition, so we cannot say anything about the profile or thickness of this layer of matter. This has to be done with another measurement which is discussed later in this report (paragraph 6.2). Also is clearly observable that the deposition with higher laser power is larger than the one with a lower laser power (see paragraph 4.1).

4.3 Deposition size for different concentrations of matter

One of the parameters that are to be studied is the concentration of matter dissolved in the solution. The chosen concentrations PVPS are $5\,wt\%$, $10\,wt\%$ (the overall used concentration) and $15\,wt\%$. But when measuring with the $5\,wt\%$ PVPS solution some problems were encountered. This solution wasn't viscous enough to hold out the whole measurement, like water as is discussed in paragraph 3.2, so the results couldn't be compared to the results of the $10\,wt\%$ and the $15\,wt\%$ measurements. The liquid would dewet from the sides before a proper measurement could be performed.

We deliberately decided not to use higher concentrations due to heat absorption of the particles. This could result in unwanted processes like igniting them. An example is shown in figure (19) where a dust particle in ethylene glycol absorbs the laser heat and ignites on a moving substrate.

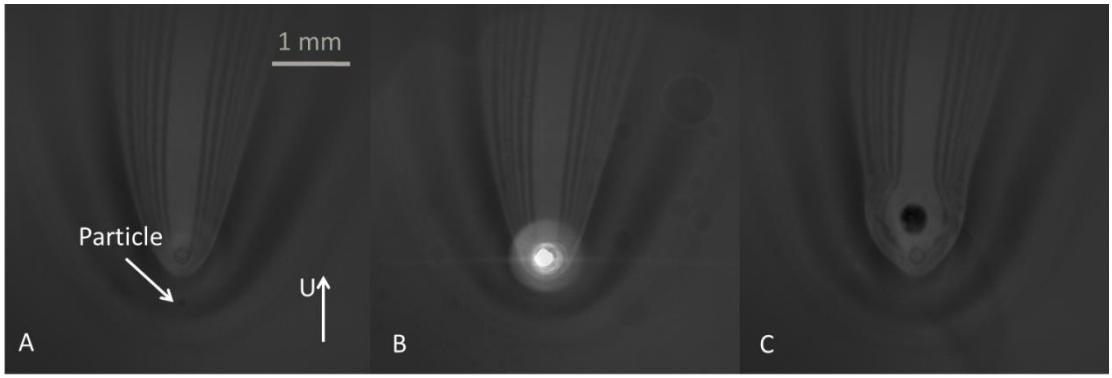

Figure 19: Laser burning a dust particle in 1EG at a laser power of 4000 mW and a speed of motion of 2,93 mm/s.

The results for the $10\,wt\%$ and $15\,wt\%$ solutions are shown in figure (20).

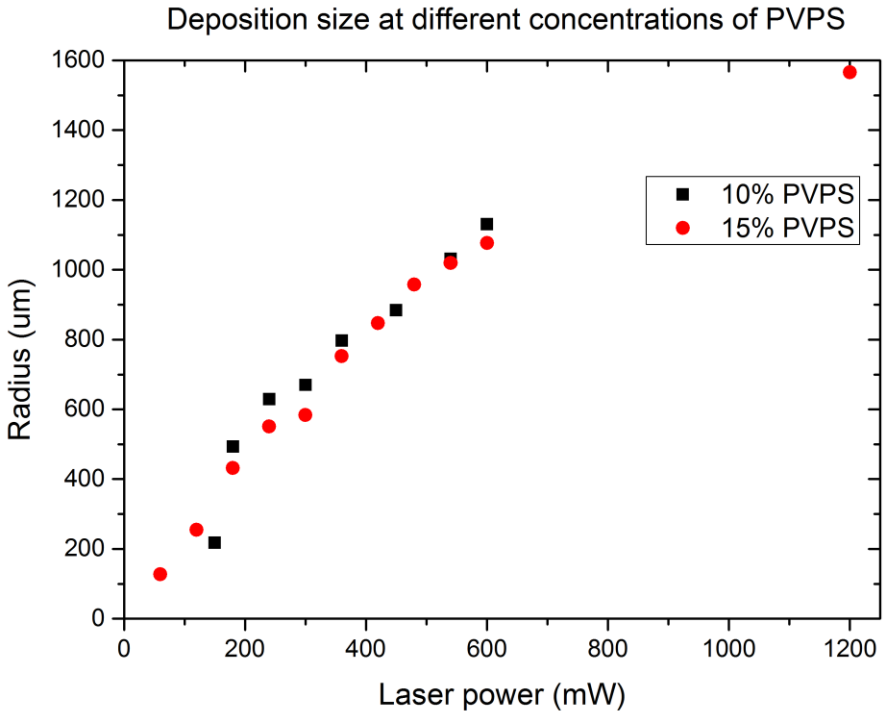

Figure 20: Compared results for the radius of the deposition plotted against the laser power for a 10% and 15% PVPS solution.

From these results we can derive that the concentration difference between 10% and 15% doesn't seem to have an (a great) influence.

4.4 Deposition size as function of time

A typical experiment for a stationary substrate is illustrated in the panels in figure 15. We can see that the deposition of matter grows over time.

The radius of this deposition is calculated and plotted as a function of time, (the time $t = 0$ coincides with switching on the laser). This is done for different laser powers, initial film thicknesses and concentrations. In figure (21) we can see a typical result.

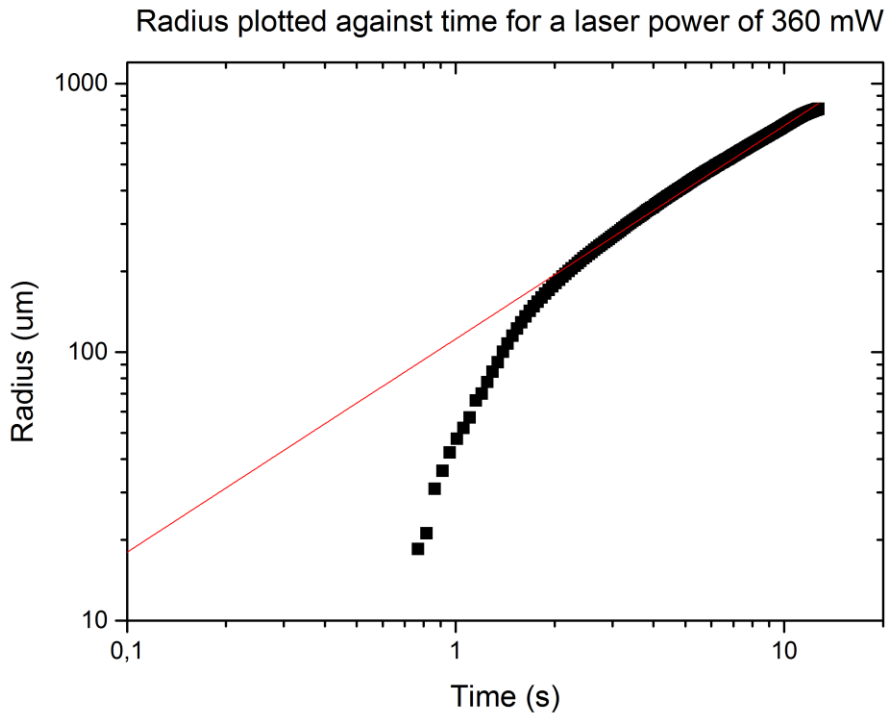

Figure 21: Deposition radius against the time for a laser power of 360 mW and a 10 wt% PVPS solution. A powerlaw fit has been calculated through the results. The fit through the results is $R=111{,}95t^{0{,}794}$.

The fit (figure 21) through the measurement results, that are plotted on a logarithmic scale, is a powerlaw fit $R = at^b$. These give values for the exponent b between $0{,}63757$ and $0{,}84709$ for laser powers between $180\,mW$ and $600\,mW$ and spin-coating rpm between $750\,rpm$ and $2000\,rpm$. These values don't seem to be in relation with any of the studied parameter so the spread is seen as a measurement uncertainty. The mean of this exponent is $b = (0{,}725 \pm 0{,}104)$. The next thing noticed from the results is that the beginning of the process shows a steeper slope for a short time, some sort of start-up growth. The origin of this phenomenon is still unclear, in this short time interval there can't be seen any strange behavior on the recordings. It could be that the determination script of deposition doesn't work fully correct in this start-up range, but this isn't verified.

Some results of the different parameters that are studied and compared are shown in the following pictures. First some results at different laser powers are shown.

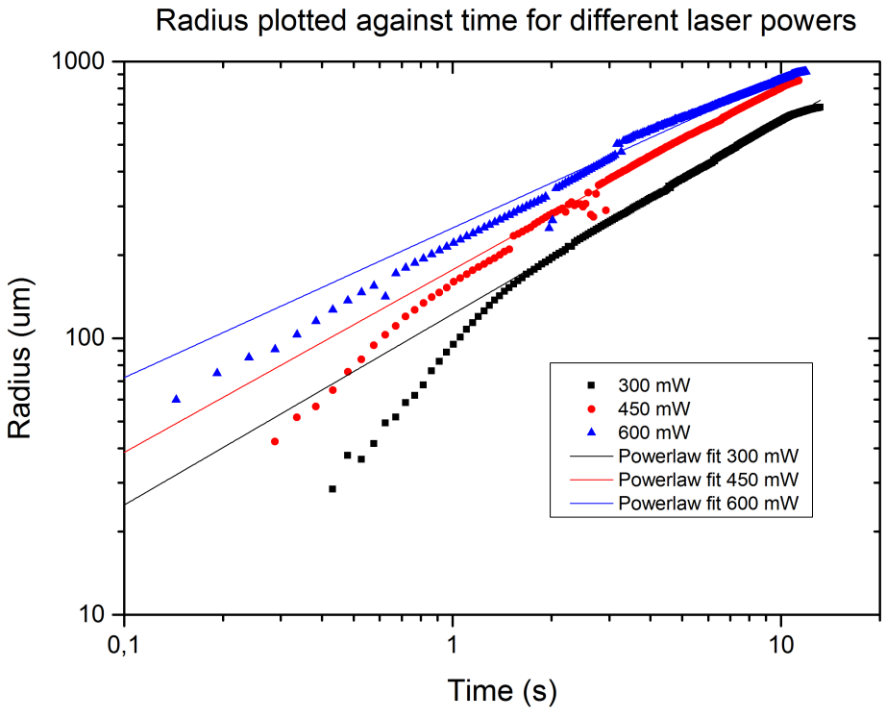

Figure 22: Deposition radius as function of time for different laser powers (300 mW, 450 mW, 600 mW). The powerlaw fit through the results are $R=122{,}27t^{0{,}69}$, $R=176{,}81t^{0{,}66}$ *and* $R=250{,}40t^{0{,}54}$ *for respectively 300 mW, 450 mW and 600 mW.*

The following figures show the radius plotted against the time for two different laser powers ($P = 180\,mW$ and $360\,mW$) with 10 $wt\%$ and 15 $wt\%$ PVPS.

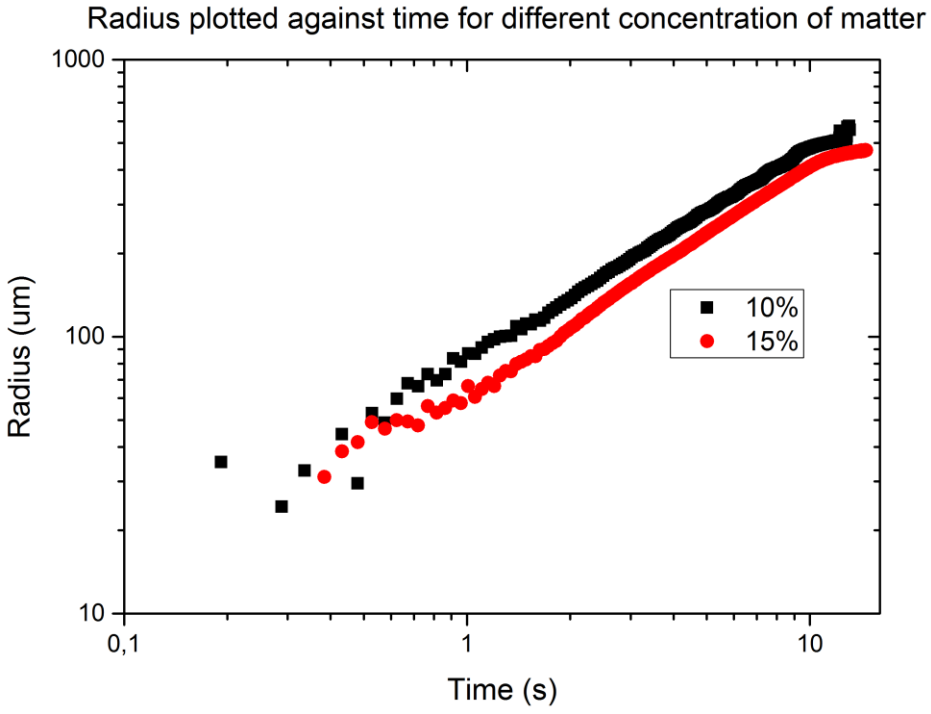

Figure 23: Deposition radius as function of time for a 10% and 15% PVPS solution and at a laser power of 180 mW.

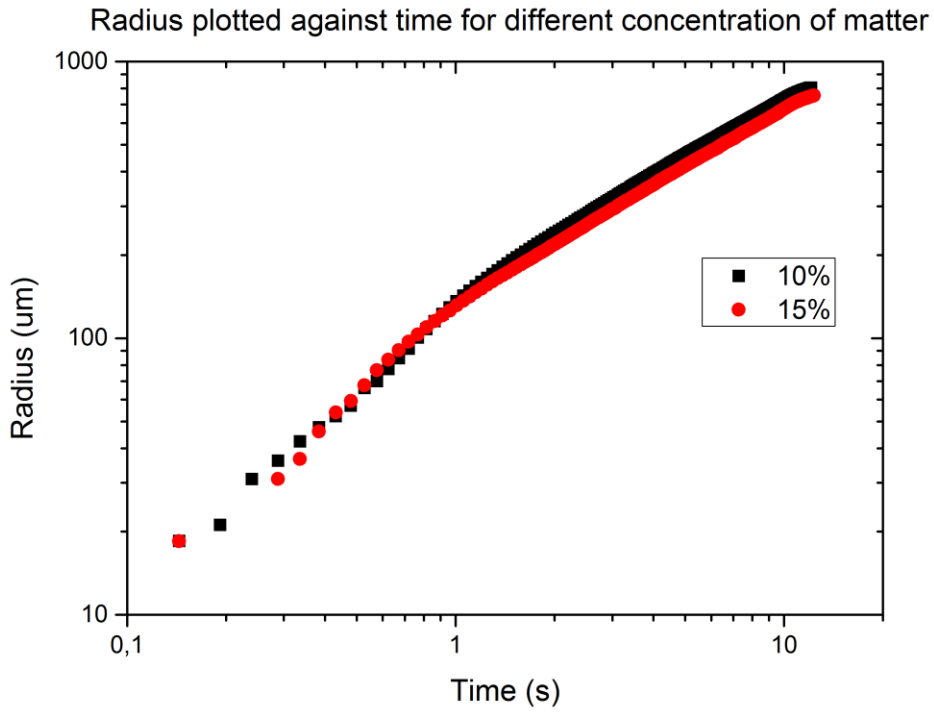

Figure 24: Deposition radius as function of time for a 10 wt% and 15 wt% PVPS solution and at a laser power of 360 mW.

We can see a recurring shape in the results. The start of the growth has a steeper slope than the slope seen in the biggest part of the measurement. Also for a higher laser power the actual deposition starts earlier. Previously, in paragraph 4.3, we saw that a concentration difference from 10% to 15% doesn't seem to bring a great difference to the end result. This also seems to be the case for the time-dependent measurement if we look at figures (23) and (24).

In paragraph 4.1 we found that at very low power the deposition didn't follow the linear relation. And if we look at the results from the measurement at $150\ mW$ and $180\ mW$, shown in figures (25) and (26), we can see a clear difference.

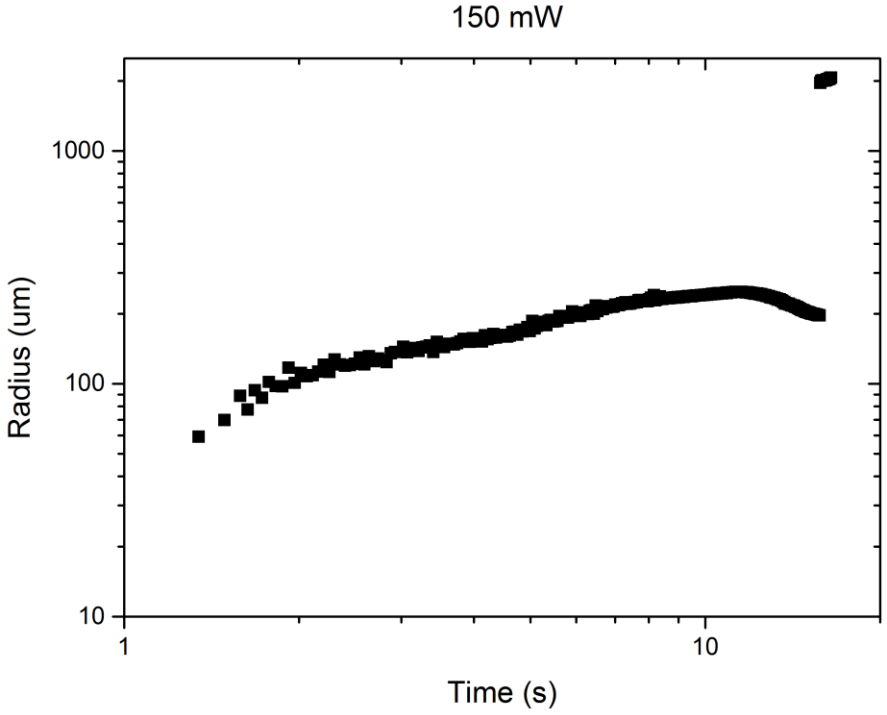

Figure 25: Plot of the radius against the time for a 10 wt% PVPS solution and at a laser power of 150 mW. The discontinuity in the last measured points are an error due to the used script to determine the deposition size and have not to be considered.

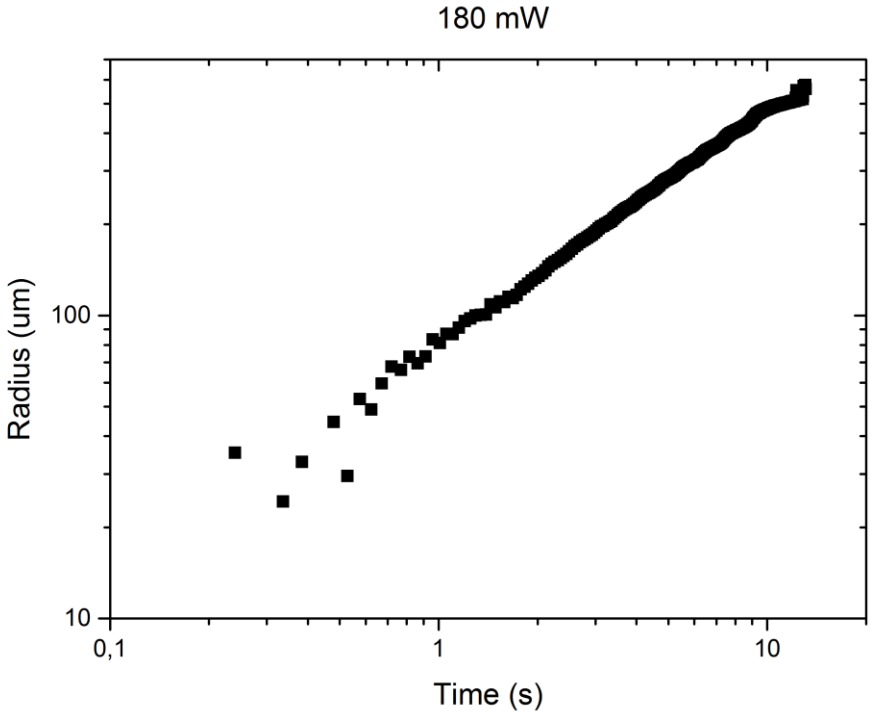

Figure 26: Plot of the radius against the time for a 10 wt% PVPS solution and at a laser power of 180 mW.

The measurement at 180 mW (figure 26) follows approximately the typical form, here the start-up growth has occurred and fulfilled. At the 150 mW measurement (figure 25) we don't see the two clear regimes, this can be explained that the 10 second laser treatment isn't even long enough for this particular laser power to fulfill the start-up growth. After these 10 seconds it even seems that the deposition size diminishes again for a small amount. We could say a limit for which a controlled deposition can occur for these parameters (spin-coating: 2 seconds on 1500 rpm and a concentration of 10% PVPS) is a minimum laser power somewhere between 150 mW and 180 mW.

The next results are for different initial film thicknesses, or more precisely different spin-speeds. Figures 27 and 28 show the plots at respectively 180 mW and 450 mW.

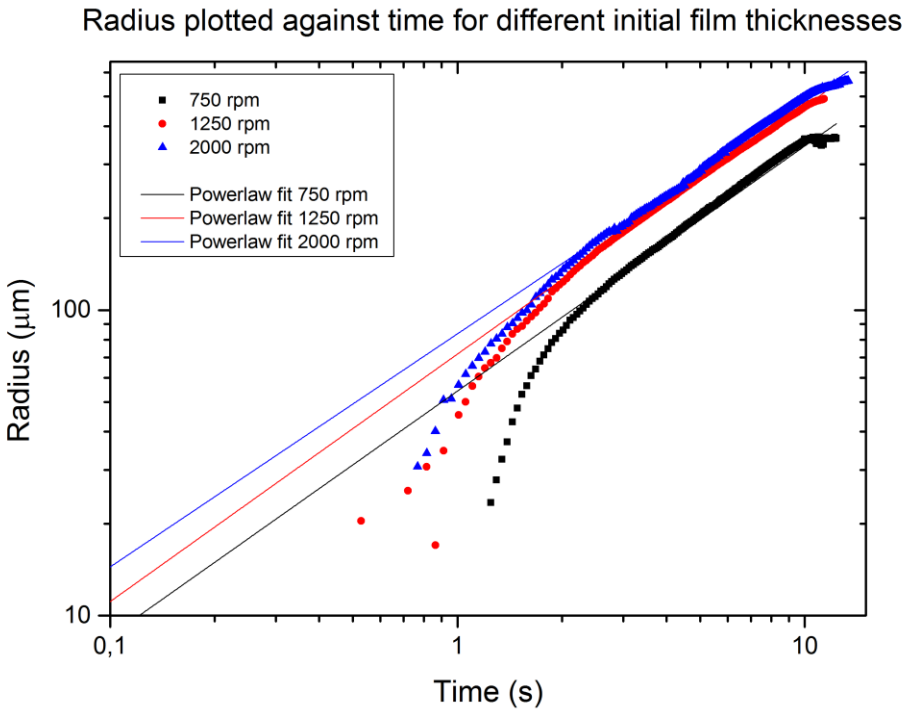

Figure 27: Deposition radius as function of time at a laser power of 180 mW for different spin-speeds ω = 750 rpm, 1250 rpm, and 2000 rpm for a 10 wt% PVPS solution. The powerlaw fits though these results are $R=54{,}34t^{0{,}80}$, $R=71{,}81t^{0{,}81}$ and $R=83{,}64t^{0{,}76}$ for respectively 750 rpm,1250 rpm and 2000 rpm.

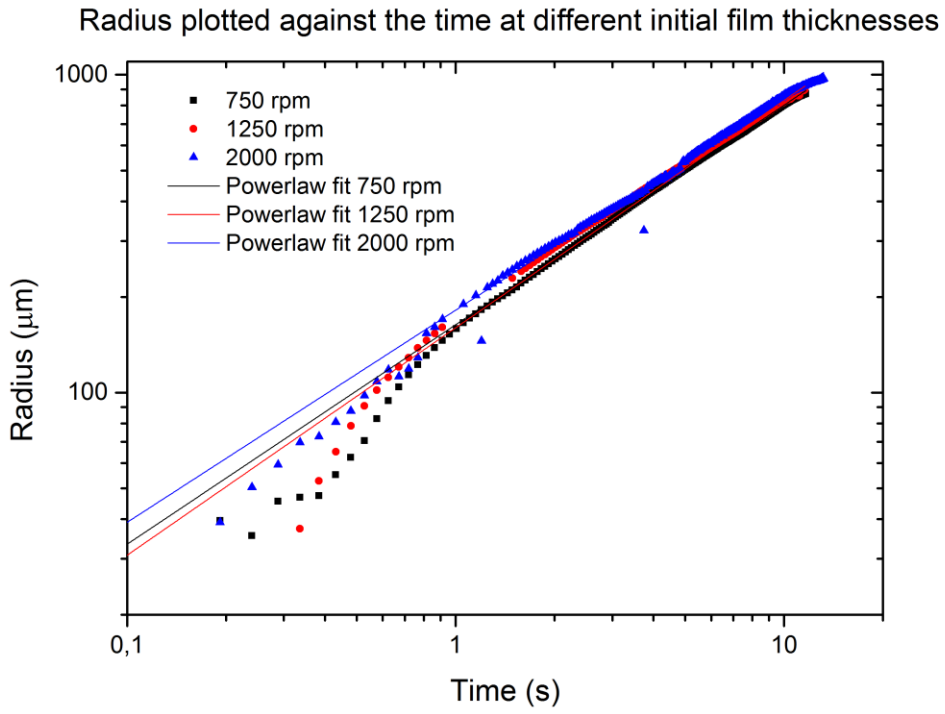

Figure 28: Plot of the radius against the time at a laser power of 450 mW for different spin-speeds $\omega = 750$ rpm, 1250 rpm, and 2000 rpm for a 10 wt% PVPS solution. The powerlaw fits though these results are $R=163{,}56t^{0{,}69}$, $R=159{,}88t^{0{,}72}$ and $R=181{,}73t^{0{,}67}$ for respectively 750 rpm,1250 rpm and 2000 rpm.

For the film thickness parameter we can't really say it has a great influence on the deposition size and process in the experimented regime. The only clear difference is the result of the measurement at $180\,mW$ (figure (27)) and a spin-coating rpm of $750\,rpm$. Although the results follow the typical form the total deposition size seems to be a bit smaller than the rest. So here the effect, discussed in paragraph 4.2, is to be perceived.

5 Deposition of matter on a moving substrate

The next step is to see if we can deposit matter in a way like writing on paper, already mentioned in the abstract part of this report. This is to be achieved by moving the substrate underneath the laser spot, this process is depicted in figure 5. The laser spot is put a distance $r = 14\,mm$ out of the center of the spin axis whereby we can calculate the actual moving speed of the substrate after we fixed the spinning revolutions per minute ω after the spin-coating process. This is easily calculated by $U = 2\ \cdot \pi \cdot r \cdot \frac{\omega}{60}$, with U the eventual movement speed.

Here the solution used is also the $10\,wt\%$ PVPS in water on mass base. A typical result where a track of PVPS is deposited on the polycarbonate plate is shown below in figure 29.

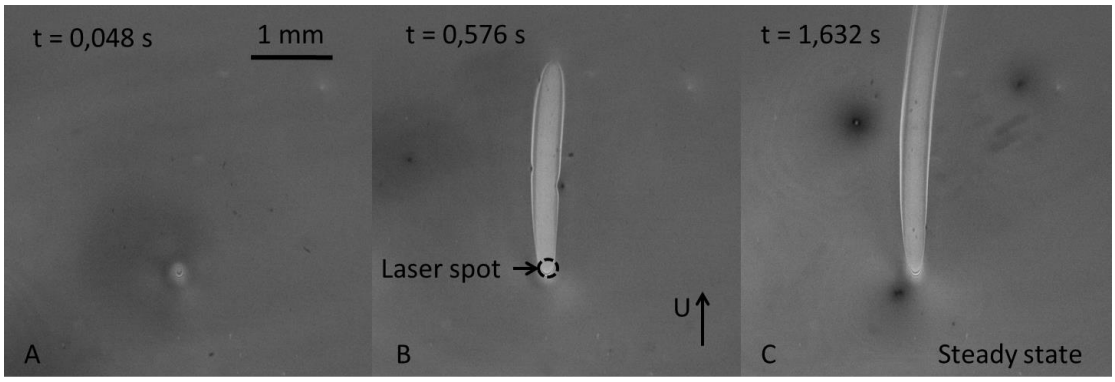

Figure 29: Image sequence of the process of deposition on a moving substrate. Here the laser power is 2400 mW and the substrate speed is U= 4,40 mm/s.

We are going to look at the track width of the deposition at the points where a steady state has occurred during the measurement. This is done for at least 5 different places on a single track.

5.1 Deposition track width as function of movement speed

First the movement speed of the substrate is being varied and its influence studied. The speed varies between $2\,mm/s$ and $7\,mm/s$ and the laser power is held constant at $2400\,mW$. Now the track width is plotted against the movement speed on a logarithmic scale and is shown in figure 30.

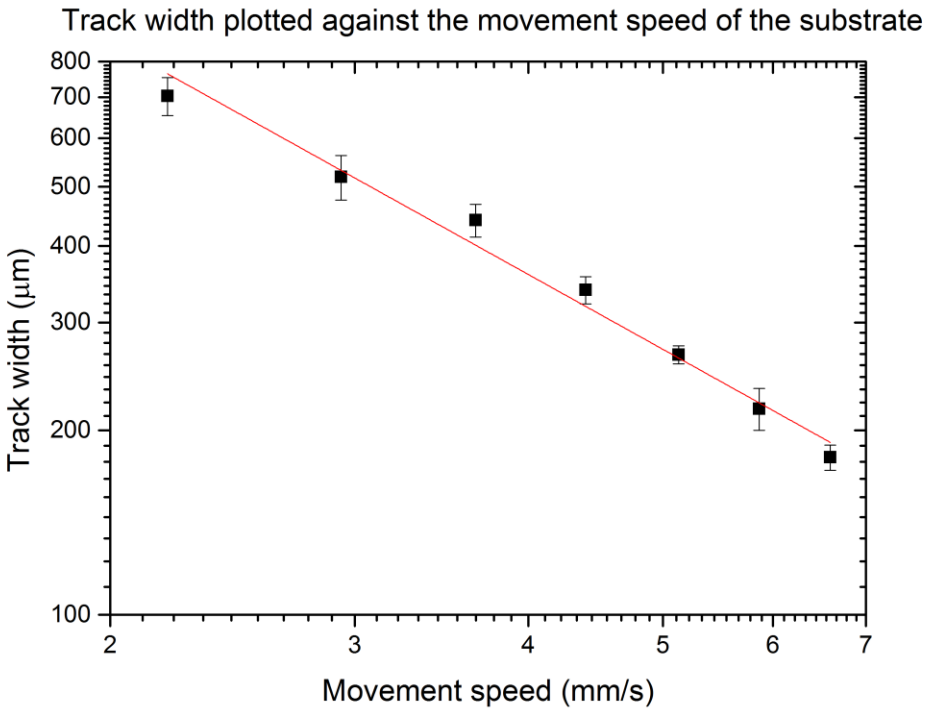

Figure 30: Track width as function of the substrate speed. The laser power is 2400 mW. The fit through the results is w=2065,09U$^{-1,26119}$.

The track width decreases with increasing movement speed. Now a fit has been plotted through the results of the form $w = aU^b$. We could suspect that this exponent of decrease is linear, so $b = -1$, because doubling the substrate speed leaves half the time for heating. Although it comes near this value, namely $b = -1{,}26119$, the difference can be explained that the heating spreads from the laser spot and therefor the next spot is already a bit heated before direct heating from the laser spot. Also the viscosity depends on temperature, so this quantity is altered by the experiment.

5.2 Deposition track width as function of laser power

Next we studied the influence of the laser power on the track width. The laser power is varied between $1920\ mW$ and $4000\ mW$. We expect that the width will increase with increasing laser power, because there will be more heat and thus more deposition. The substrate speed is held constant at around $4{,}4\ mm/s$. The results are shown in figure 31.

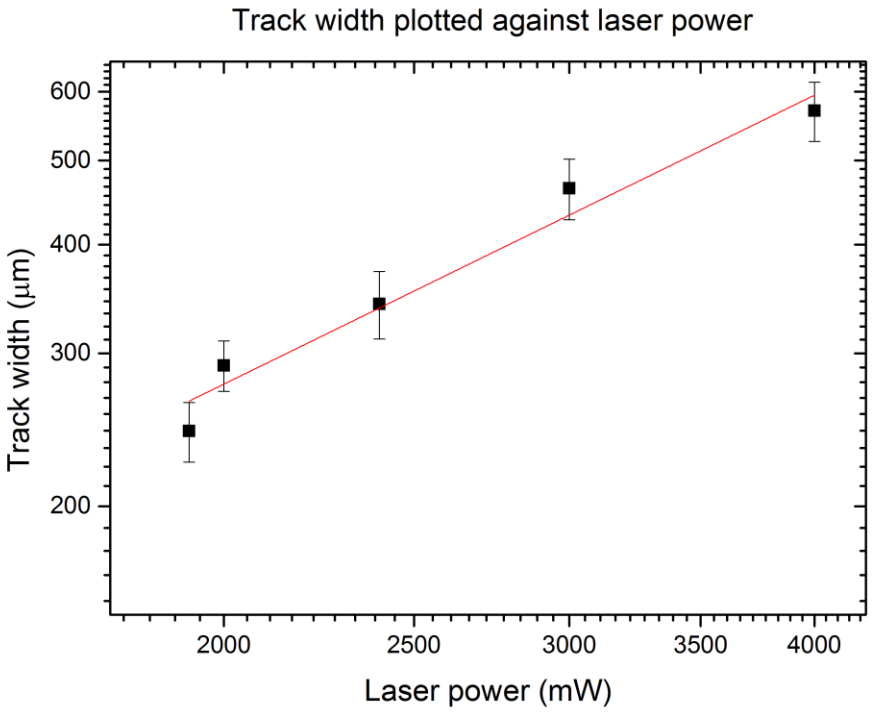

Figure 31: Track width as function of laser power on a moving substrate, the movement speed is 4,40 mm/s. The fit through the results is $w=0{,}06P^{1{,}10468}$.

Again, the expectance is correct and a fit has been plotted through the results of the form $w = aP^b$. Here the exponent is $b = 1{,}10468$ which almost equals 1 so the influence seems linear.

5.3 Deposition track width as function of initial film thickness

For the reason given in paragraph 4.2 we cannot measure the absolute film thickness but can relate the thickness to the spin-speed. These are inversely proportional related to each other. The spin-speed varied between $750\,rpm$ and $2000\,rpm$, such that the initial film thickness will vary around $4\,\mu m$ and $14\,\mu m$. Laser power and substrate speed are held constant at respectively $2400\,mW$ and $4{,}4\,mm/s$. The track width is plotted against the spin-coating rpm in the figure 32 below.

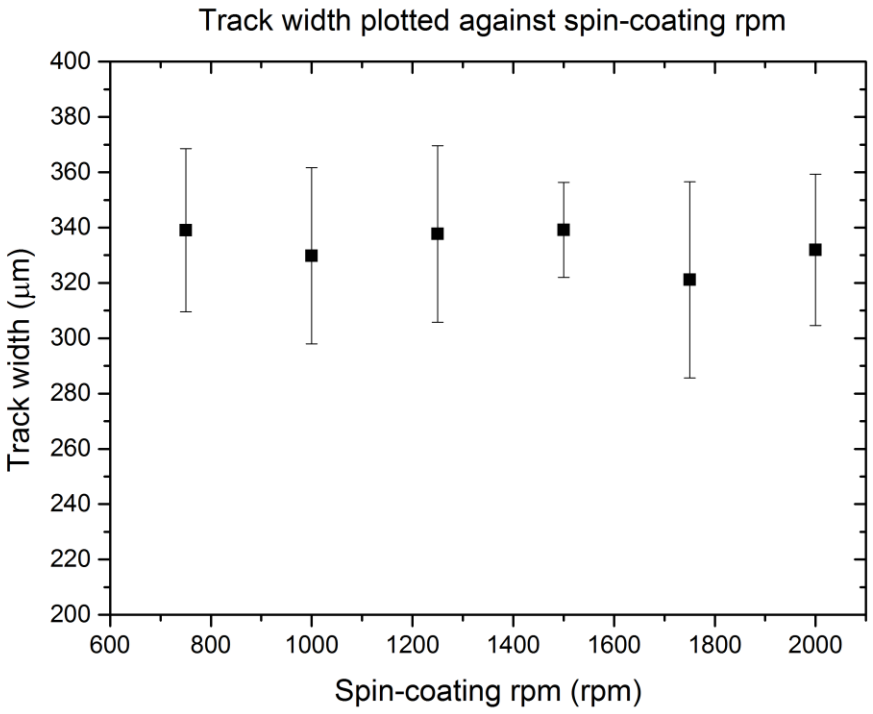

Figure 32; Track width as function of the spin-speed. The laser power is 2400 mW and the substrate speed 4,40 mm/s.

The results show that the film thickness, in the tested regime, doesn't seem to affect the track width. On a stationary substrate an increase in size could be observed, but the influence wasn't very big. Here the substrate isn't heated for 10 seconds on the same spot but moved, so it seems that the influence of the film thickness grows with the time it is being heated.

5.4 Deposition track width for different concentrations of matter

Last the concentration is altered to observe the influence. We don't expect any big influence since it had almost none on the stationary substrate. A concentration of $15\ wt\%$ PVPS is used and because the same reason as before a concentration of $5\ wt\%$ PVPS can't last long enough for a proper regime of parameter variation. In the experiments the laser power $(2400\ mW)$ and film thickness are kept constant. The movement speed is varied so the results can be compared to that of paragraph 5.1, these are plotted together in figure 33.

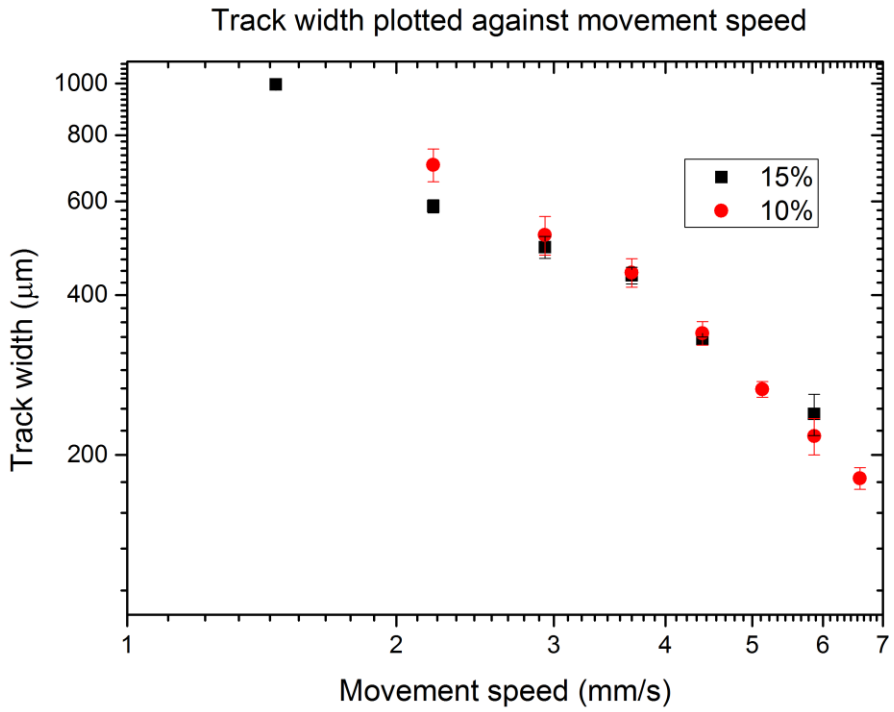

Figure 33: Track width as function of the substrate speed for a 10 wt% and 15 wt% PVPS solution. The laser power is 2400 mW.

As before we see that a concentration of $10\ wt\%$ or $15\ wt\%$ doesn't seem to affect the deposition width. The only observable difference is that a concentration of $15\ wt\%$ PVPS is a bit more viscous. Thus we can measure at slower substrate speeds because, although we don't see a difference in track width the spontaneous dewetting of the substrate is delayed.

6 Experiments without explicit results

There have been some more experimental ideas on this subject that were carried out. But in practice it turned out not to give useful results. The two subjects that were supposed to be carried out were: determining the profile of the deposited matter and using another dissolved matter. The latter was supposed to be PEDOT:PSS, one of the active matters in for example OLED screens. In the next sections the outcomes and problems are discussed.

6.1 PEDOT:PSS

PEDOT:PSS or Poly(3,4-ethylenedioxythiophene) Polystyrene sulfonate is, as mentioned before, an electrically conductive polymer and one of the active materials in OLED screens.

The mixture available and used for our experiments were water based. The percentage of PEDOT:PSS was no more than 1% and thereby had a low viscosity. This leads to some difficulties in the experiments on a hydrophobic substrate. If looked back at the results from paragraph 3.2 it is to be observed that water has a much lower rupture time, what is less viscous than ethylene glycol. If we want to study the deposition on a stationary substrate we can't measure an appropriate length of time for the laser to be on. And when we measure on a moving substrate there is only a very limited regime where we can measure until a steady state has formed. An example of a, maybe, useable measurement is showed in figure (34).

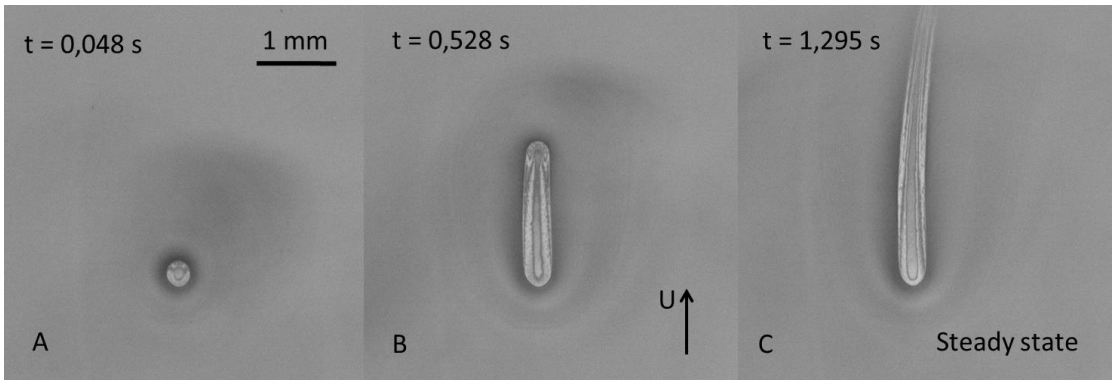

Figure 34: Image sequence of a measurement on a moving substrate with a PEDOT:PSS solution where steady state has been reached.

But most measurements didn't go as well as the previous. An example is shown in figure (35).

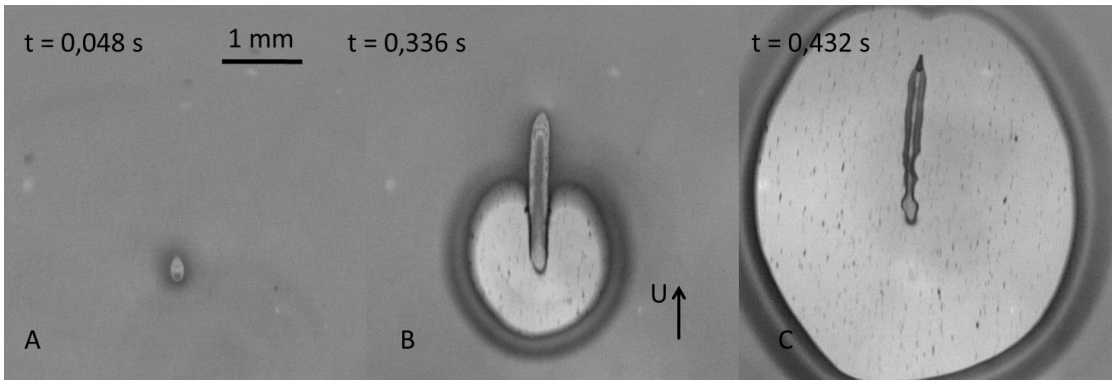

Figure 35: Image sequence of an unusable measurement.

With these problems occurring and a time limit for this project there hasn't been any time to remedy this particular experiment. No useful results could be obtained or compared to the results from the PVPS measurements.

6.2 Profile determination

Profile determination already has been mentioned in paragraph 4.2. here we saw that the deposition size increases with decreasing initial film thickness. The size measured is in a 2D perspective, this *x-y* plane is the surface of the substrate, so we couldn't say anything about the thickness and profile of the deposition.

The intention was to do this with an absorption measurement. The substrate with deposition pattern had to be placed above an inverted microscope, now the light was falling through from above the substrate. The image observed by the microscope should be of a lower intensity where the light had to travel through the deposition pattern and the substrate. The set-up is depicted in figure (36).

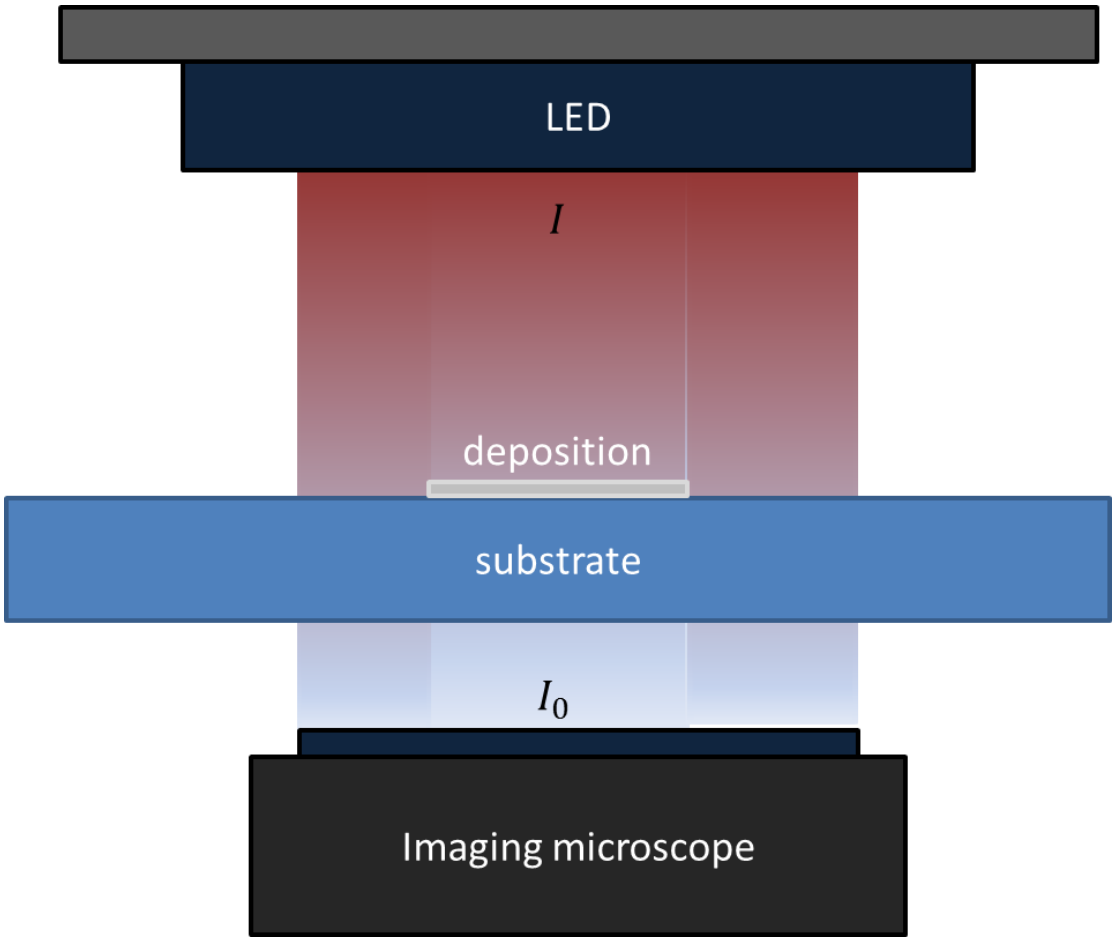

Figure 36: Schematic image of the absorption measurement.

Now the local thickness of the deposition could be determined by using the relation of intensity I before and after absorption. Due to this absorption this leads to[8] the Beer-Lambert law:

$$I = I_0 \mathrm{e}^{-\gamma d} \tag{8}$$

Here I is the measured intensity, I_0 the incoming intensity of the light, γ the absorption coefficient of the matter of deposition and d is this thickness of the layer. The absorption of the substrate has be subtracted like background. Eventually the equation can be rewritten for an expression for the thickness of the deposition:

$$d = \frac{1}{\gamma}\ln(I_0 \backslash I). \tag{9}$$

All this would work well in theory, but the reality shows that there is almost no difference in intensity after the light went through the substrate or through deposition and substrate. It has been tried with 3 different light sources with three different wavelengths. The layer of deposition is just too thin that absorption is minimal and the microscope can't measure any difference. It could be expected that this would cause some trouble because we spin-coat layers between $4\,\mu m$ and $14\,\mu m$ from a solution with a maximum of $15\,wt\%$ PVPS. So the thickest layer would be estimated around $2{,}1\,\mu m$. But the most experiments were done at thinner initial thicknesses and a concentration of $10\,wt\%$ PVPS, these leave a layer too thin for an absorption measurement.

The measurements have been done in this regime of film thickness without any further notice of this particular experiment. So the deposition layers were too thin for this experiment to determine their profiles.

7 Summary, conclusion and further research

7.1 Summary and conclusions

The goal of this project was study the behavior of the deposition process with help of a laser. This is done for a stationary and a moving substrate and a parameter variation study has been carried out on a solution of PVPS in water. The results will be discussed in the following paragraphs. For all following results the laser was on for 10 seconds.

First of all the experiments on a stationary substrate were carried out. If we look at the process over time we can see a recurring development. First there is a small time interval, about a second, when actual deposition is started where the size increases faster than during the rest of the process.

Next the influence of laser power is studied. For this we can say that with increasing laser power there is an increase in size, defined as the radius of the deposition. The tested regime is from $60\,mW$ to $600\,mW$, the initial film thickness is kept at a constant height. We can say that at a certain minimum laser power there is actual deposition and for another value of laser power the process of deposition is past the aforementioned start-up phenomenon. At the tested laser powers we can say that, for this initial film thickness, actual deposition starts at somewhat below $150\,mW$ and the steady process is reached at around $180\,mW$.

Furthermore the initial film thickness is altered and the laser power is kept constant, first at $180\,mW$ and another time at $450\,mW$. For both laser powers we can observe that this influence of initial film thickness is much more insignificant than that of the laser power. There could be an increase of deposition observed with decreasing thickness but this spread in radius of deposition is about $100\,\mu m$ where that of the laser power was about $1000\,\mu m$. There is also the fact that at a thinner film thickness a thinner deposition layer is somewhat expected, but the profile measurements on the depositions couldn't be carried out. So there can only yet be said that the radius of the deposition doesn't seem strongly influenced by the initial film thickness.

Also the concentration of the solution is looked upon. In the previous experiments the concentration of PVPS in water was 10% on mass base. Now, due to experimental reasons, only a concentration of 15% is also used for measurements. For this difference in concentration no difference can be seen in size of deposition.

The next big difference is the use of a moving substrate. Here the movement speed of the substrate is another variable. The influence of this parameter is that for increasing movement speed we see an decrease of deposition track width. The tested regime is from $1{,}47\,mm/s$ till $6{,}60\,mm/s$ and the initial film thickness and laser power ($2400\,mW$) have been kept constant. We can see that from around $2{,}20\,mm/s$ there is actual deposition on the substrate. The increase in track width seems fairly linear, deviation can be explained by the dependency of material constants to temperature.

Again the laser power has been altered for the experiments and we can see a similar relation. By increasing the laser power the track width will also increase. Furthermore, we see the same relation for the concentration difference of 10% and 15%. This is that these tested concentrations don't bring any difference in track width.

But now the difference in initial film thickness doesn't seem to have any effect on the deposition. The track width doesn't change for initial spin-coating settings of *2* seconds on *750* rpm to *2000* rpm what causes differences between initial film thickness h_0 and 37,5% of h_0.

7.2 Further research

There is always room for improvement and expansion. In this project some of these could be, for example, measuring in a broader range of parameters like laser power or substrate speed. Also developing a numerical model for this process of deposition would be useful to rationalize the experimental results.

Some expansions on the tested influences could accurately determine the boundaries of the laser power or substrate speed where actual deposition starts. Additionally, also the boundaries where the deposition process isn't steady anymore, what is defined as the limit at which dewetting will occur before the process is completed (figure 16), could be determined.

But there were also some experiments tried during this project where improvement is needed. One of these is the use of PEDOT:PSS as dissolved material so we can deposit this polymer, used as charge carrier, on a substrate. The problem with this solution was that, for the tried regimes, no steady measurement series could be performed. The mixture used wasn't viscous enough for hydrophobic substrates. A solution could be, using a mixture with a higher percentage of PEDOT:PSS. Also some more variables could be altered to see if a steady regime can be found to do these experiments. Due to the time limit of this project this hasn't yet been done excessively.

An extensive experiment based on different dissolved materials could also be a useful project. By this, the characteristics of a material could be coupled to some of the already studied parameters.

The last example, already tried before, is determining the profile of the deposited materials. An inventory of substrates with deposition are still waiting for a more accurate absorption measurement technique or another method like an electron microscope. In the following figures some depositions or shown. These images are taken through a microscope.

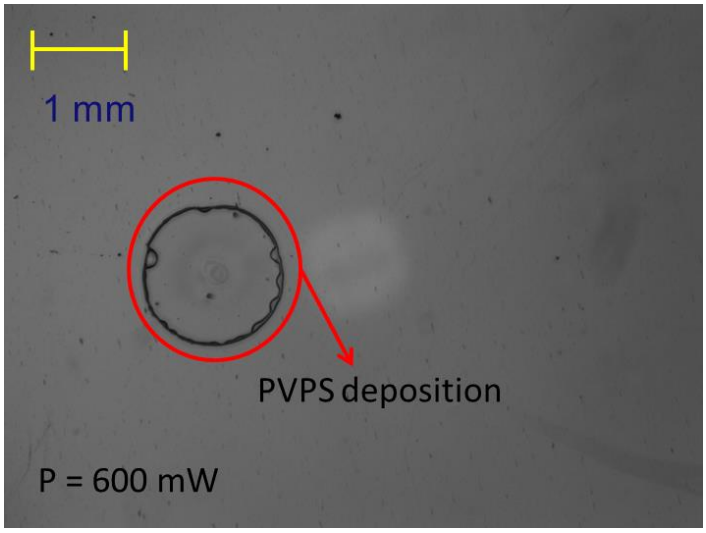

Figure 37: Microscopic image of the deposition left behind from an experiment. Here the laser was on for 10 seconds with a power of 600 mW. There is still a thin liquid line to be seen on the boundaries of the deposition spot left behind by the dewetting process.

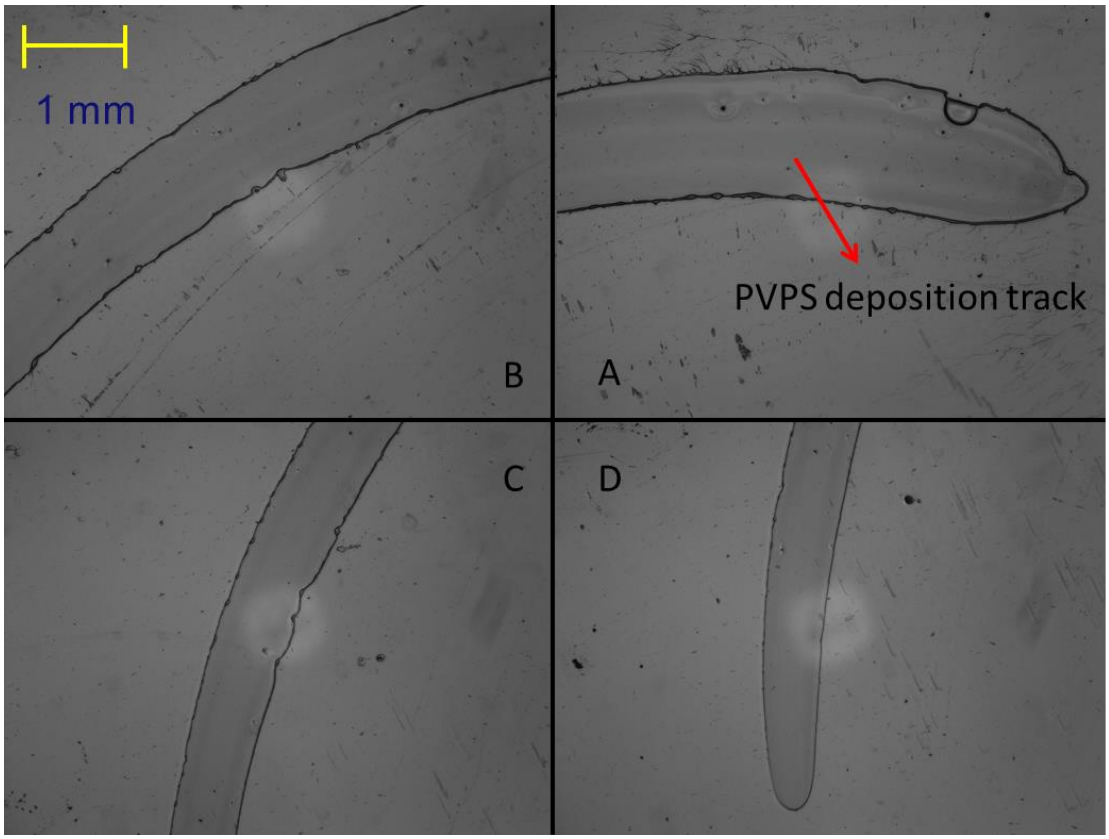

Figure 38: Microscopic image sequence of the deposition track from an experiment. Here image A to D give the order from the start until the end of the measurement. The dewetting started at the end of panel D, we can still see a liquid edge at the start of the deposition in panel A what is left behind by the dewetting process.

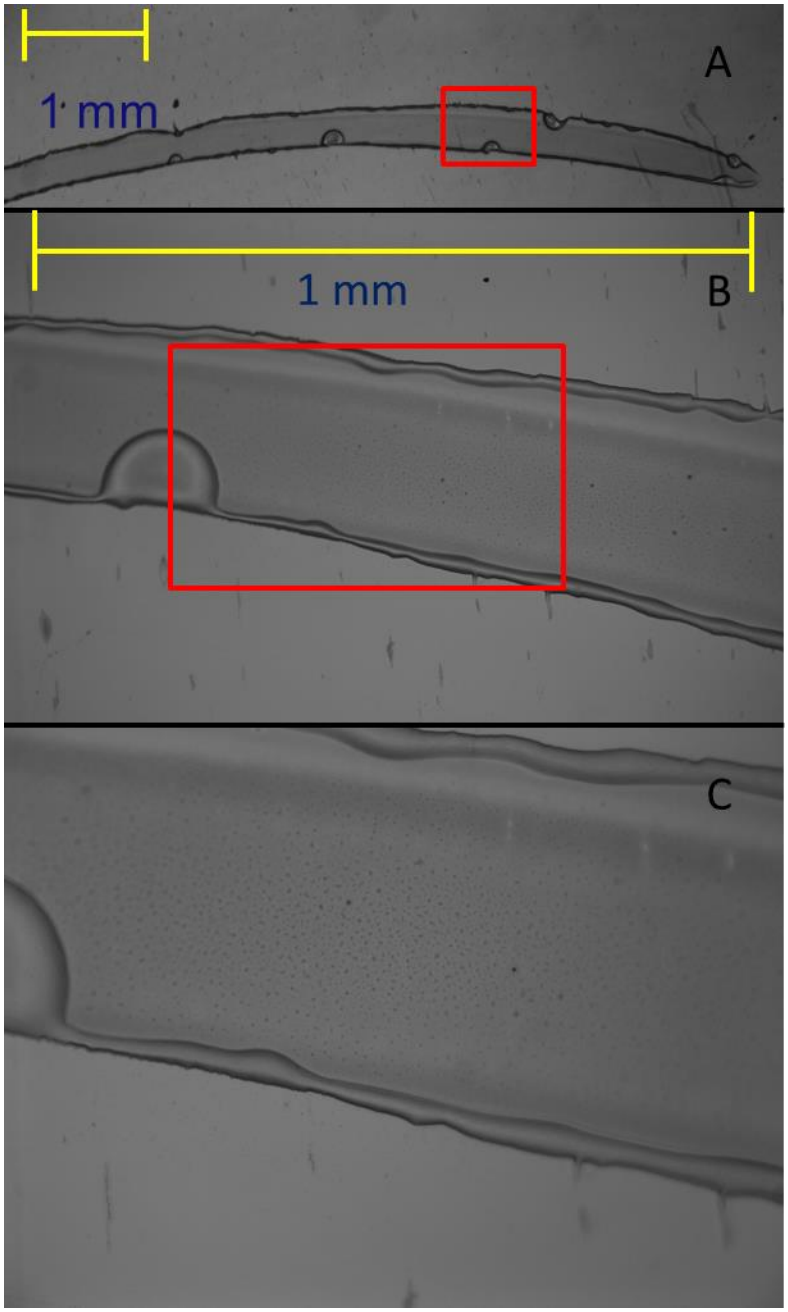

Figure 39: Microscopic images of a single part of the deposition track. Here panel A has a relative magnification of 2x, panel B a magnification of 10x and panel C 20x. Thus when we zoom in we can see particles in the deposited track. Also some darker and lighter areas can clearly be observed so it doesn't seem a uniform distribution. This is why a profile determination of the deposition would be a nice further research subject.

8 References

[1] Guang-Feng Wang: *Fabrication and characterization of OLEDs using PEDOT:PSS and MWCNT nanocomposites*, Nanotechnology Centre, Institute of Textiles and Clothing, The Hong Kong Polytechnic University, Hong Kong, 2007.

[2] N. R. Bieri: *Microstructuring by printing and laser curing of nanoparticle solutions*, Laboratory of Thermodynamics in Emerging Technologies, Department of Mechanical and Process Engineering, ETH Zurich, 2003

[3] N. R. Bieri: *Manufacturing of nanoscale thickness gold linesby laser curing of a discretely deposited nanoparticle suspension*, Laboratory of Thermodynamics in Emerging Technologies, Department of Mechanical and Process Engineering, ETH Zurich, 2004.

[4] V. A. Kochemirovsky: *Laser-Induced Copper Deposition with Weak Reducing Agents*, Department of Chemistry, Saint-Petersburg University, 2013.

[5] Edward M. Nadgorny, Jaroslaw Drelich: *Laser-Based Deposition Technique: Patterning Nanoparticles into Microstructures*, Michigan Technological University, Houghton, Michigan, U.S.A., 2014.

[6] H.M.J.M Wedershoven, C.W.J Berendsen, J.C.H Zeegers, A.A. Darhuber: *Thermocapillary deformation of thin liquid films by infrared irradiation*, Technische Universiteit Eindhoven, 2013.

[7] A.G. Emslie, F.T. Bonner, L.G. Peck: *Flow of a viscous liquid on a rotating disk*, J. Appl. Phys.

[8] Oxford Dictionary of Biochemistry and Molecular Biology (2 ed.): Beer-Lambert law